# A Novel Memcapacitor and Its Application in a Chaotic Circuit

**Mei Guo**
Shandong University of Science and Technology
**Ran Yang**
Shandong University of Science and Technology
**Meng Zhang**
Shandong University of Science and Technology
**Renyuan Liu**
Shandong University of Science and Technology
**Yongliang Zhu**
Shandong University of Science and Technology
**Gang Dou** ( dougang521@163.com )
Shandong University of Science and Technology

**Research Article**

**Keywords:** Memcapacitor, memristor, chaotic circuit, multistability

**Posted Date:** March 4th, 2021

**DOI:** https://doi.org/10.21203/rs.3.rs-221899/v1

**Noname manuscript No.**
(will be inserted by the editor)

# A novel memcapacitor and its application in a chaotic circuit

**Mei Guo · Ran Yang · Meng Zhang · Renyuan Liu · Yongliang Zhu · Gang Dou**

Received: date / Accepted: date

**Abstract** In this paper, a novel memcapacitor is designed by SBT memristor and two capacitors. A fifth-order memcapacitor and memristor chaotic circuit is proposed. The stability of the equilibrium point of the system is analyzed theoretically. Lyapunov exponents spectra, bifurcation diagrams, poincaré maps and phase diagrams are used to analyze the dynamic behaviors of the system. The results show that under different initial values and parameters, the system produces rich dynamic behaviors such as stable points, limit cycles, chaos, and so on. Specially, coexisting attractors, transient chaos, and steady-state chaos accompanied by burst period phenomenon are also produced in the system. The proposed memcapacitor-based circuit expands the research methods of memcapacitor for application in chaotic circuits.

**Keywords** Memcapacitor · memristor · chaotic circuit · multistability

## 1 Introduction

Chua predicted the existence of memristor based on mathematical relations between pairs of fundamental circuit variables in 1971 [1]. HP laboratory made the first solid-state thin film memristor in 2008 [2]. A memristor is a nonlinear two-terminal circuit element reflecting the relationship between magnetic flux and charge ($\varphi$-$q$). Chua and co-workers further proposed memcapacitor based on memristor, which further expanded the concept of memory elements [3, 4]. Memcapacitor is a passive two-terminal electronic device described by the non-linear constitutive relationship of magnetic flux and the time-domain integral of electric charge $q$ ($\varphi$-$\sigma$). Memcapacitor or memristor can easily generates high-frequency chaotic oscillation signals in the circuit because of the characteristic of nonlinearity, and many chaotic circuits introduced them to obtain chaos [5–9]. The chaotic circuits can generate some unique phenomena, including transient chaos [10–13], steady-state chaos accompanied by burst period phenomenon [14], and multistable phenomenon [15–18].

The behaviors of different memcapacitor models [19–25] are explored through previous researches on memcapacitor. Ref. [19] described a synthesis of mutators which can transform the emulated memristor into memcapacitor and meminductor. Ref. [20] converted a digital memristor into memcapacitor by virtue of the voltage following characteristics of operational amplifiers, which complicated the memcapacitor model. Ref. [21] presented a memcapacitor simulator based on an LDR memristor and constructed a memcapacitor model. Ref. [22] designed a floating memcapacitor emulator, the circuit structure was simple and can be widely used in circuit design. Recently, researches based on memcapacitor have become a focus [26–28]. In Ref. [26], a fractional order memcapacitor model was proposed and a chaotic oscillator based on the model was investigated. Ref. [27] proposed a logarithmic charge-controlled memcapacitor model and verified it non-volatility and switching features. These simulating memcapacitors were mostly based on complex conversion circuit, which were prone to errors, and it is not easy to the analysis of the characteristics of the memcapacitor. Therefore, it is necessary to find a new way to study the application of memcapacitor.

A memcapacitive device can be implemented by appending a memristor with a MIM capacitor in Ref. [29]. As the resistance of memristor changes, the capacitance of memcapacitor changes under external excitation. This structure

Mei Guo · Ran Yang · Meng Zhang · Renyuan Liu · Yongliang Zhu · Gang Dou
College of Electrical Engineering and Automation,
Shandong University of Science and Technology, Qingdao 266590, China
E-mail: dougang521@sdust.edu.cn

has a potential for the CMOS technology, artificial neural networks, and chaotic circuits. Based on the method of constructing physical memcapacitor proposed by Ref. [29], this paper uses the physical SBT ($Sr_{0.95}Ba_{0.05}TiO_3$) memristor [30, 31] in our lab to design a memcapacitor, which can be directly used as a circuit element to generates chaos in the circuit. This paper constructs a fifth-order chaotic circuit composed of memcapacitor and memristor.

The paper is organized as follows. In Sect. 2, the dynamical modeling of the fifth-order memcapacitor and memristor chaotic circuit is introduced and its corresponding plane equilibrium and stability are analyzed. In Sect. 3, the influences of initial states and circuit parameters on system dynamic behaviors are studied. The conclusions are drawn in Sect. 4.

## 2 Dynamical modeling of the chaotic circuit based on memcapacitor and SBT memristor

### 2.1 The chaotic circuit based on memcapacitor and SBT memristor

In the previous researches, the mathematical model of the memristor had been proposed [30,31]. According to the experimental measurement of the memristor, the flux-controlled model of the memristor was obtained as follows:

$$\begin{cases} i(t) = (A + B|\varphi(t)|)u(t) \\ \frac{d\varphi(t)}{dt} = u(t) \end{cases} \tag{1}$$

where $A = 0.0676$, and $B = 0.3682$.

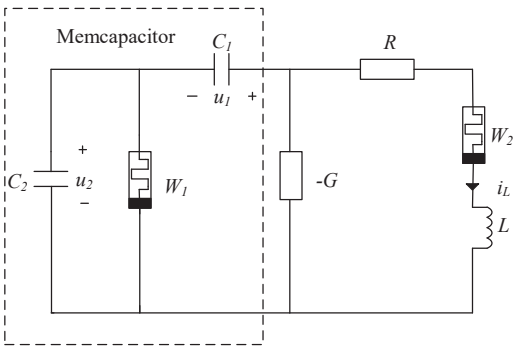


**Fig. 1** The fifth-order chaotic circuit based on the memcapacitor and SBT memristor

The fifth-order chaotic circuit based on novel memcapacitor and SBT memristor is shown in Fig. 1. The fifth-order chaotic circuit consists of a novel memcapacitor, a SBT memristor $W_2$, a resistor $R$, a negative conductance $-G$, and an inductance $L$. According to Ref. [29], the novel memcapacitor is composed of memristor $W_1$ and two capacitors ($C_1$ and $C_2$), as shown in the dotted line.

According to Kirchhoff's circuit laws, the current $i_L$ of inductor $L$, the voltage $u_1$ of capacitor $C_1$, the voltage $u_2$ of capacitor $C_2$, the magnetic flux $\varphi_1$ of memristor $W_1$ , and the magnetic flux $\varphi_2$ of memristor $W_2$ are selected as state variables, the state equations of the system as

$$\begin{cases} \frac{di_L(t)}{dt} = \frac{1}{L}\left[u_1(t) + u_2(t) - Ri_L(t) - \frac{i_L(t)}{W_2}\right] \\ \frac{du_1(t)}{dt} = \frac{1}{C_1}\left[G(u_1(t) + u_2(t)) - i_L(t)\right] \\ \frac{du_2(t)}{dt} = \frac{1}{C_1}\left[G(u_1(t) + u_2(t)) - i_L(t) - W_1u_2(t)\right] \\ \frac{d\varphi_1(t)}{dt} = u_2(t) \\ \frac{d\varphi_2(t)}{dt} = \frac{i_L(t)}{W_2} \end{cases} \tag{2}$$

Let $x = i_L(t)$, $y = u_1(t)$, $z = u_2(t)$, $w = \varphi_1(t)$, $v = \varphi_2(t)$, $a = 1/C_1$, $b = 1/C_2$, $c = 1/L$, $r = R$, and $g = G$, the dimensionless equation of the system are as follows:

$$\begin{cases} \dot{x} = c[y + z - rx - \frac{x}{W_2}] \\ \dot{y} = a[g(y + z) - x] \\ \dot{z} = b[g(y + z) - x - W_1z] \\ \dot{w} = z \\ \dot{v} = \frac{x}{W_2} \end{cases} \tag{3}$$

where $W_1$=$A + B|w|$, $W_2 = A + B|v|$.

### 2.2 Typical chaotic attractors

When the parameters are set as in Table 1, the complex dynamic behaviors occur in the system. The system generates a double-scroll attractor (see Fig. 2). By Jacobi matrix method, the five Lyapunov exponents are calculated as $LE_1$ = 0.1446, $LE_2$ = 0.01265, $LE_3$ = 0.0091, $LE_4$ = -0.2864, and $LE_5$ = -6.917. The sum of the Lyapunov exponents is negative, which mean that the system is chaotic.

**Table 1.** The system parameters for the chaotic attractor

| Parameters | $a$ | $b$ | $c$ | $r$ | $g$ |
|---|---|---|---|---|---|
| Values | 3.39 | 1.95 | 9.36 | 0.42 | 1.42 |

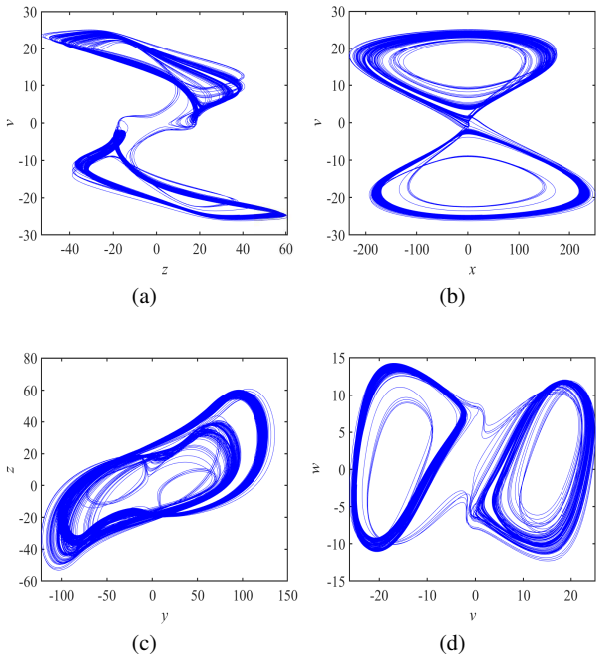


**Fig. 2** The typical chaotic attractor of fifth-order chaotic circuit

### 2.3 Plane equilibrium and stability distribution

Setting the circuit parameters as in Table 1 and letting $\dot{x} = \dot{y} = \dot{z} = \dot{w} = \dot{v} = 0$ in Eq. (3), the equilibrium point of the system can be obtained as:

$$A = \{(x,y,z,w,v) \mid x = y = z = 0, w = m, v = n\} \tag{4}$$

where $m$, $n$ are real constants. That is, the points on the $w$-$v$ plane are the equilibrium point of the system (3). The Jacobian matrix $J$ of Eq. (3) can be expressed as:

$$J = \begin{bmatrix} -cr - \frac{c}{W_2} & c & c & 0 & 0 \\ -a & ag & ag & 0 & 0 \\ -b & bg & bg - bW_1 & 0 & 0 \\ 0 & 0 & 1 & 0 & 0 \\ \frac{1}{W_2} & 0 & 0 & 0 & 0 \end{bmatrix} \tag{5}$$

The characteristic equation of the equilibrium point $A$ can be given as:

$$det(\lambda E - J) = \lambda^2(\lambda^3 + a_1\lambda^2 + a_2\lambda + a_3) = 0 \tag{6}$$

where $a_1$, $a_2$, $a_3$ are as follows:

$$\begin{cases} a_1 = bW_1 - bg - ag + cr + \frac{c}{W_2} \\ a_2 = (bcr - abg)W_1 + \frac{cbW_1 - bcg - acg}{W_2} - acrg - bcrg + ac + bc \\ a_3 = (abc - abcrg)W_1 - \frac{abcgW_1}{W_2} \end{cases} \tag{7}$$

According the Routh-Hurwitz stability criterion, if all the nonzero eigenvalues of Eq. 6 are negative, the system is stable:

$$a_1 > 0, a_3 > 0, a_1a_2 - a_3 > 0 \tag{8}$$

If $n = 0$, $m$ is a variable parameter, the conditions $a_1 > 0$, and $a_3 > 0$ in Eq. (8) cannot be satisfied simultaneously. If $m = 0$, $n$ is a variable parameter, the Eq. (8) has no solution. Obviously, the equilibrium point $A$ is always unstable. No matter where the system (3) starts, the system tends to limit cycles, chaos, or infinite divergence.

## 3 The complex dynamic behaviors of the system

### 3.1 Chaos oscillations dependent on the initial states

#### *3.1.1 Influences of initial conditions x(0), y(0), z(0), w(0), and v(0) on system chaos oscillations*

Setting the system parameters as in Table 1 and the initial values of the system as (0.001, 0, 0, 0, 0). The Lyapunov exponents spectra and bifurcation diagrams varying with the initial states $x(0)$, $y(0)$, $z(0)$, $w(0)$, and $v(0)$ are shown in Fig. 3-7. The system remains chaos oscillations with the variation of initial states.

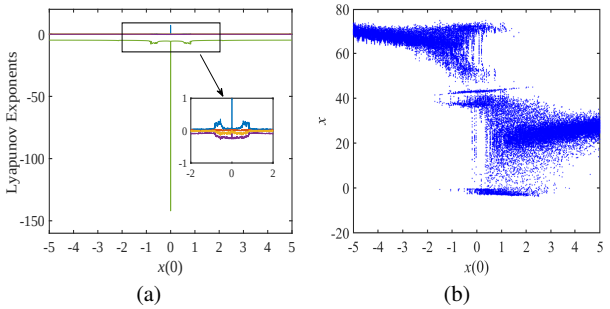


**Fig. 3 a** Lyapunov exponents spectrum and **b** bifurcation diagram varying with the initial state $x(0)$

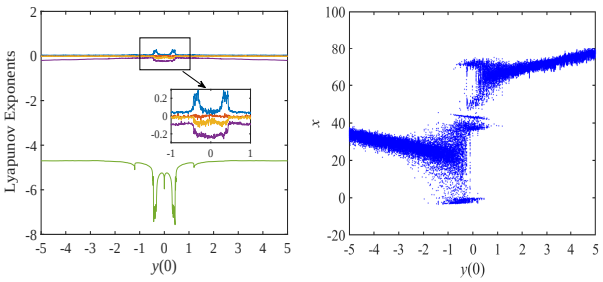


**Fig. 4** **a** Lyapunov exponents spectrum and **b** bifurcation diagram varying with the initial state $y(0)$

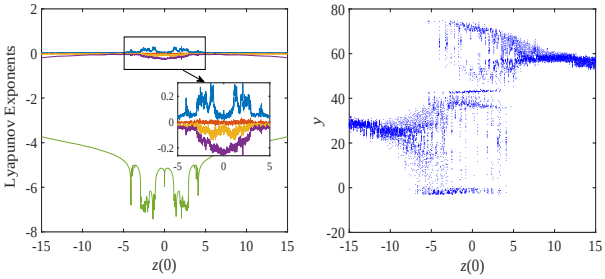


**Fig. 5** **a** Lyapunov exponents spectrum and **b** bifurcation diagram varying with the initial state $z(0)$

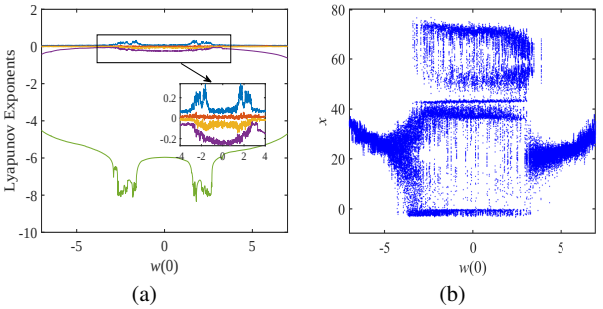


**Fig. 6** **a** Lyapunov exponents spectrum and **b** bifurcation diagram varying with the initial state $w(0)$

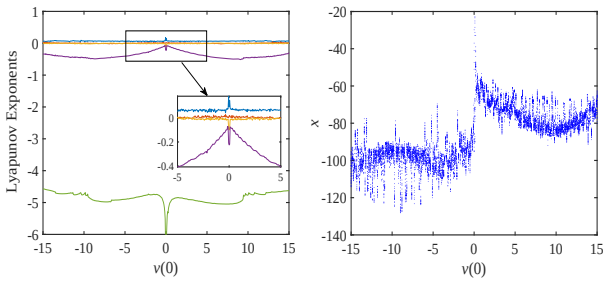


**Fig. 7** **a** Lyapunov exponents spectrum and **b** bifurcation diagram varying with the initial state $v(0)$

### *3.1.2 Multistability depending on the initial condition z(0)*

Multistability is a common characteristic in chaotic systems. Figure 8 shows the coexisting chaotic attractors and the corresponding Poincaré map. Figures 8a and b show the coexisting single-scroll chaotic attractors in detail and the corresponding Poincaré map, where the blue attractor starts from the initial conditions of (0.001, 0, 7, 0, 0) and the red one starts from (0.001, 0, -7, 0, 0). Figures 8c and d show the coexisting double-scroll chaotic attractors in detail and the corresponding Poincaré map, where the blue attractor starts from the initial conditions of (0.001, 0, 1.5, 0, 0) and the red one starts from (0.001, 0, -1.5, 0, 0). Figures 8e and f show the coexisting single-scroll chaotic attractor and double-scroll chaotic attractor in detail and the corresponding Poincaré map, where the blue attractor starts from the initial conditions of (0.001, 0, 3, 0, 0) and the red one starts from (0.001, 0, -3, 0, 0).

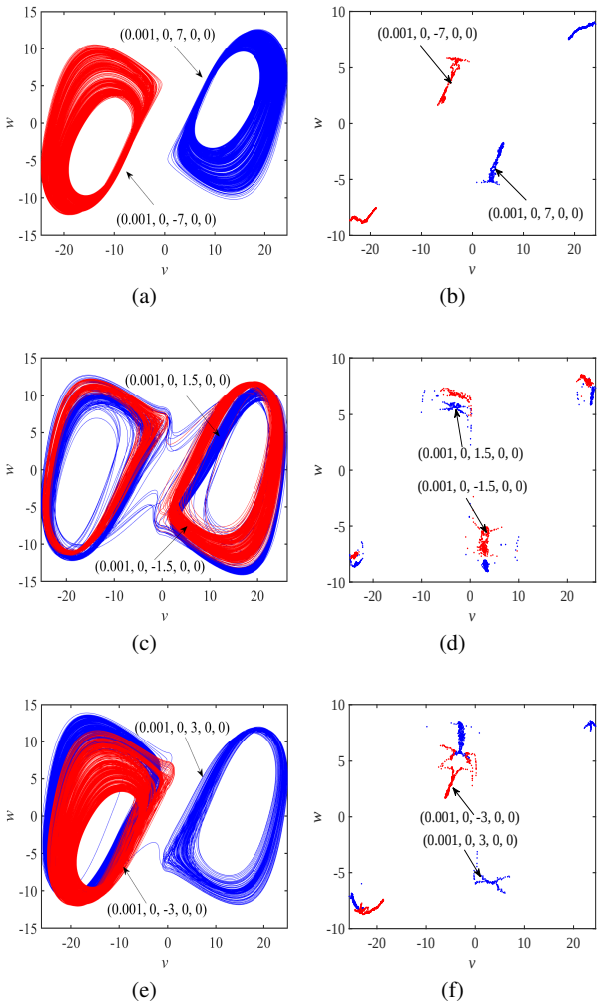


**Fig. 8** The multistability of the circuit varying with initial conditions $z(0)$. **a** the phase diagram when $z(0) = \pm 7$; **b** the Poincaré map when $z(0) = \pm 7$; **c** the phase diagram when $z(0) = \pm 1.5$; **d** the Poincaré map when $z(0) = \pm 1.5$; **e** the phase diagram when $z(0) = \pm 3$; **f** the Poincaré map when $z(0) = \pm 3$

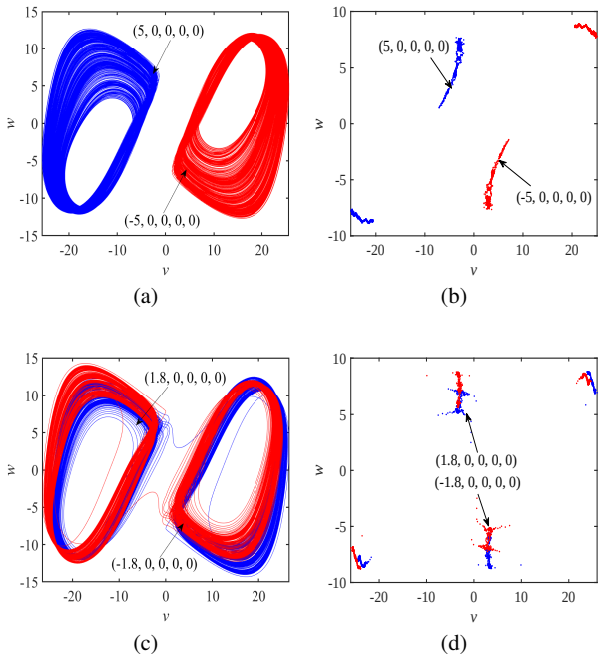


**Fig. 9** The multistability of the circuit varying with initial conditions $x(0)$; **a** the phase diagram when $x(0) = \pm 5$; **b** the Poincaré map when $x(0) = \pm 5$; **c** the phase diagram when $x(0) = \pm 1.8$; **d** the Poincaré map when $x(0) = \pm 1.8$

### *3.1.3 Multistability depending on the initial conditions x(0), y(0), w(0), and v(0)*

Other initial conditions can also produce coexisting chaotic attractors. Taking the circuit parameters as in Table 1, the phase diagrams and the Poincaré maps of the multistability dependent on the initial conditions $x(0)$, $y(0)$, $w(0)$, and $v(0)$ are shown in Fig. 9-12 , the results are summarized in Table 2.

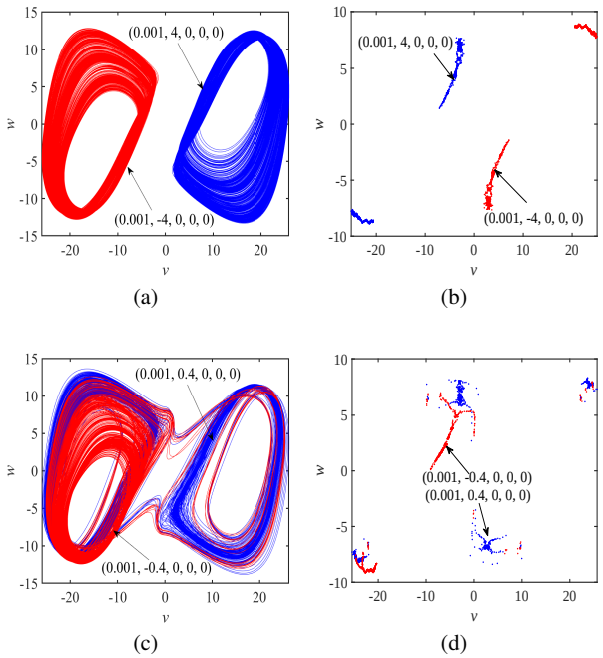


**Fig. 10** The multistability of the circuit varying with initial conditions $y(0)$; **a** the phase diagram when $y(0) = \pm 4$; **b** the Poincaré map when $y(0) = \pm 4$; **c** the phase diagram when $y(0) = \pm 0.4$; **d** the Poincaré map when $y(0) = \pm 0.4$

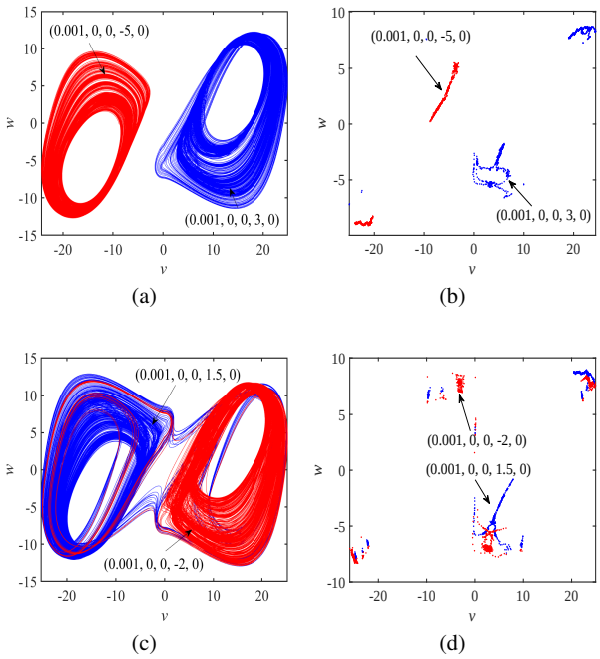


**Fig. 11** The multistability of the circuit varying with initial conditions $w(0)$. **a** the phase diagram when initial conditions are (0.001, 0, 0, 3, 0) and (0.001, 0, 0, -5, 0); **b** the Poincaré map when initial conditions are (0.001, 0, 0, 3, 0) and (0.001, 0, 0, -5, 0); **c** the phase diagram when initial conditions are (0.001, 0, 0, 1.5, 0) and (0.001, 0, 0, -2, 0); **d** the Poincaré map initial conditions are (0.001, 0, 0, 1.5, 0) and (0.001, 0, 0, -2, 0)

**Table 2.** The multistability of the circuit and corresponding initial conditions in Fig. 9-12

| Figure | Initial conditions | Coexisting attractors |
|---|---|---|
| Figure 9a, b | (±5, 0, 0, 0, 0) | Single-scroll |
| Figure 9c, d | (±1.8, 0, 0, 0, 0) | Double-scroll |
| Figure 10a, b | (0.001, ±4, 0, 0, 0) | Single-scroll |
| Figure 10c, d | (0.001,±0.4, 0, 0, 0) | Double-scroll |
| Figure 11a, b | (0.001, 0, 0, 3, 0) and (0.001, 0, 0, -5, 0) | Single-scroll |
| Figure 11c, d | (0.001, 0, 0, 1.5, 0) and (0.001, 0, 0, -2, 0) | Double-scroll |
| Figure 12a, b | (0, 0, 0, 0, ±5) | Single-scroll |

## 3.2 Dynamic behaviors dependent on system parameters

### *3.2.1 Influences of parameter a on system dynamic behaviors*

When parameter $a$ is in the range of [1.50, 3.80] and initial values are (0.001, 0, 0, 0, 0), the Lyapunov exponents spectrum and bifurcation diagram can be obtained, as shown in Fig.13. In order to better observe the Lyapunov exponents of the chaos, the fifth Lyapunov exponential curve is not drawn . When $a$ is in the range of [1.50, 1.81], the system is stable; when $a$ is in the range of [1.82, 3.67], the system exhibits chaotic attractors; when $a$ is in the range of [3.68, 3.80], system exhibits limit cycles. The dynamical evolution process of the system with the change of parameter $a$ is shown in Fig.14, where the values of $a$ are 3.22, 3.39, and 3.70, respectively.

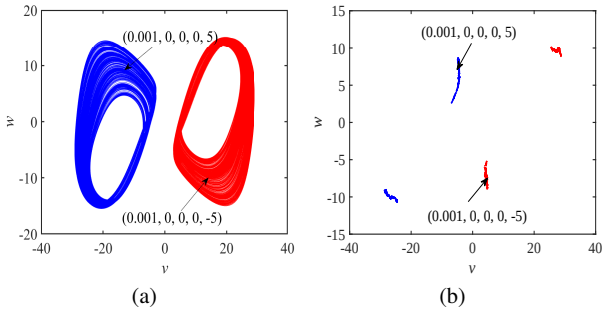


**Fig. 12** The multistability of the circuit varying with initial conditions $v(0)$. **a** the phase diagram when $v(0) = \pm 5$; **b** the Poincaré map when $v(0) = \pm 5$

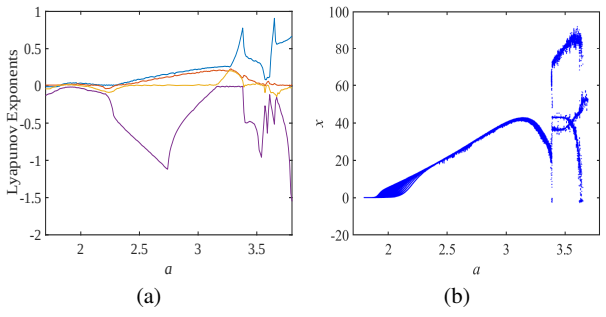


**Fig. 13** **a** Lyapunov exponents spectrum and **b** bifurcation diagram varying with the system parameter $a$

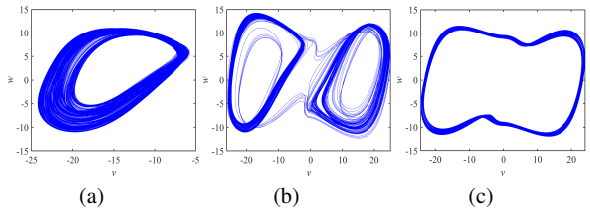


**Fig. 14** The dynamical evolution process of the system with the variety of parameter $a$. **a** $a = 3.22$; **b** $a = 3.39$; **c** $a = 3.70$

When parameter $a$ is in the range of [1.50, 3.80], and others are set as in Table 1. Dynamical behaviors with coexisting bifurcation diagrams are presented in Fig. 15, where the trajectories colored in the blue start form the initial conditions (0.001, 0, 0, 0, 0), and those colored in red correspond to (0, 0.001, 0, 0, 0). When parameter $a = 3.22$, the coexisting signal-scroll chaotic attractors in detail and the corresponding Poincaré map are shown in Fig. 16, where the blue attractor starts from the initial conditions of (0.001, 0, 0, 0, 0) and the red one starts from (0, 0.001, 0, 0, 0).

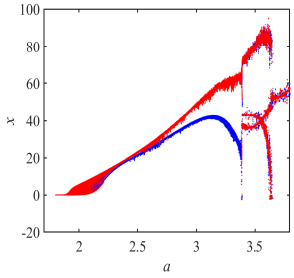


**Fig. 15** The coexistence bifurcation diagrams of parameter $a$ with the initial values (0.001, 0, 0, 0, 0) and (0, 0.001, 0, 0, 0)

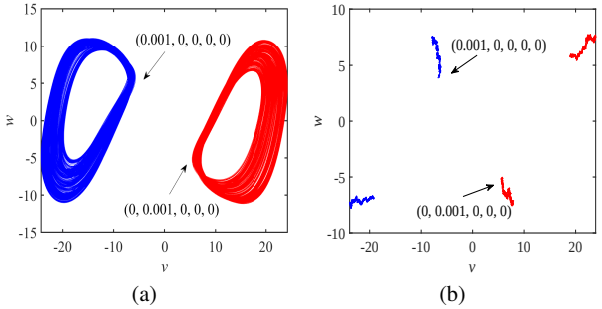


**Fig. 16** The coexisting signal-scroll chaotic attractors plotted for $a = 3.22$. **a** the phase diagram when initial values are (0.001, 0, 0, 0, 0) and (0, 0.001, 0, 0, 0); **b** the Poincaré map when initial values are (0.001, 0, 0, 0, 0) and (0, 0.001, 0, 0, 0)

### *3.2.2 Influences of parameter c on system dynamic behaviors*

Letting parameter $c$ is in the range of [9.00, 14.00], and the others are set as in Table1. When the initial values are (0.001, 0, 0, 0, 0), the Lyapunov exponents spectrum and bifurcation diagram can be obtained, as shown in Fig. 17. In order to better observe the Lyapunov exponents of the chaos, the fifth Lyapunov exponential curve is not drawn . When parameter $c$ is in the range of [9.00, 13.37] the system is chaotic, while in the range of [13.38, 14.00], the system is stable.

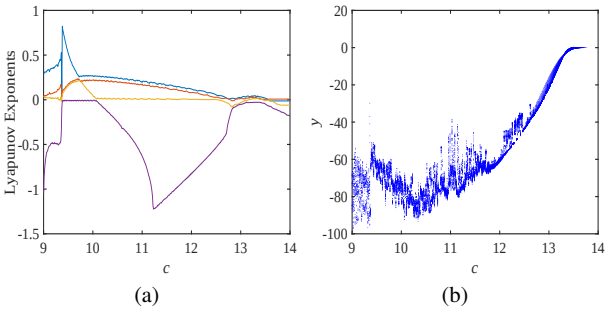


**Fig. 17** **a** Lyapunov exponents spectrum and **b** bifurcation diagram varying with the system parameter $c$

Dynamical behaviors with coexisting bifurcation diagrams are presented in Fig. 18, where the trajectories colored in the blue start from the initial conditions (0.001, 0, 0, 0, 0), and those colored in red correspond to (-0.001, 0, 0, 0, 0). When parameter $c = 9.76$, the coexisting signal-scroll chaotic attractors in detail and the corresponding Poincaré map are shown in Fig. 19, where the blue attractor starts from the initial conditions of (0.001, 0, 0, 0, 0) and the red one starts from (-0.001, 0, 0, 0, 0).

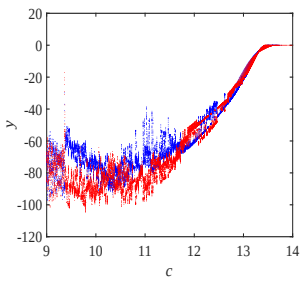


**Fig. 18** The coexistence bifurcation diagrams of parameter $c$ with the initial values (0.001, 0, 0, 0, 0) and (-0.001,0, 0, 0, 0)

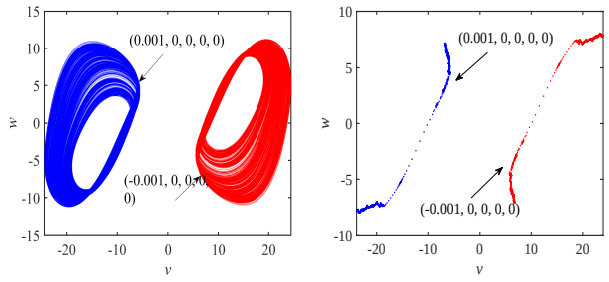


**Fig. 19** The coexisting signal-scroll chaotic attractors plotted for $c = 9.76$ and initial conditions are $(\pm 0.001, 0, 0, 0, 0)$. **a** the phase diagram; **b** the Poincaré map

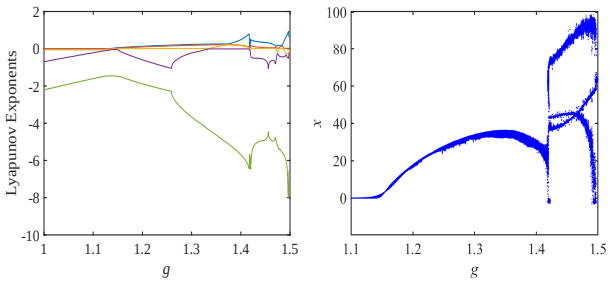


**Fig. 22** **a** Lyapunov exponents spectrum and **b** bifurcation diagram varying with the system parameter $g$

### *3.2.3 Influences of parameters b, r, and g on system dynamic behaviors*

Setting the initial values of the system as (0.001, 0, 0, 0, 0), the Lyapunov exponents spectra and bifurcation diagrams with the variation in system parameters $b$, $r$, and $g$ are shown in Fig. 20-22. The dynamics of the chaotic circuit are shown in Table 3.

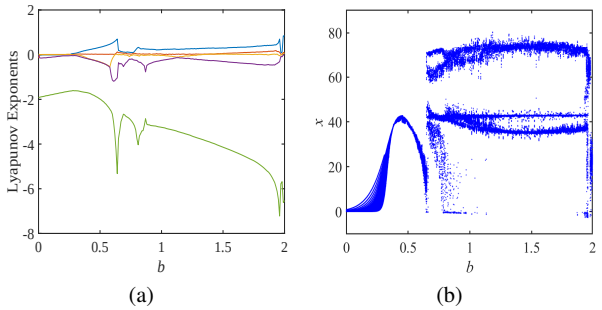


**Fig. 20** **a** Lyapunov exponents spectrum and **b** bifurcation diagram varying with the system parameter $b$

**Table 3.** The dynamics with the variation in system parameters $b$, $r$, and $g$

| System parameters | Interval | Dynamics |
|---|---|---|
| $b$ | [0.00, 0.32] | Stable point |
| | [0.33, 0.64] | Single-scroll attractor |
| | [0.65, 2.00] | Double-scroll attractor |
| $r$ | [0.30, 0.35] | Limit cycle |
| | [0.36, 0.42] | Double-scroll attractor |
| | [0.43, 0.50] | Single-scroll attractor |
| $g$ | [1.00, 1.14] | Stable point |
| | [1.15, 1.40] | Single-scroll attractor |
| | [1.41, 1.50] | Double-scroll attractor |

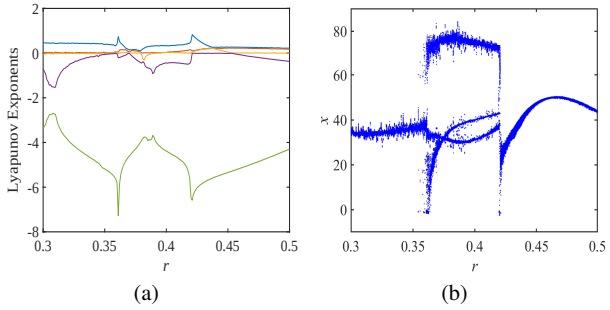


**Fig. 21** **a** Lyapunov exponents spectrum and **b** bifurcation diagram varying with the system parameter $r$

## 3.3 Transient chaos

Taking the initial values of the system as (0.001, 0, 0, 0, 0) and $b = 1.97$, other parameters remain unchanged. In the finite time range, the chaotic phenomenon of the system is transient chaos. The phenomenon of transient chaos accompanied by boundary crisis are often encountered in dynamic systems. As shown in Fig. 23, with the state variable $v$ changing in the time range [20 s, 360 s] and [380 s, 1000 s], the system produces different dynamic phenomena. When $t \in [20s, 360s]$, the system behaves as single-scroll attractors. As time goes by, when $t \in [380s, 1000s]$, the system behaves as double-scroll attractors.

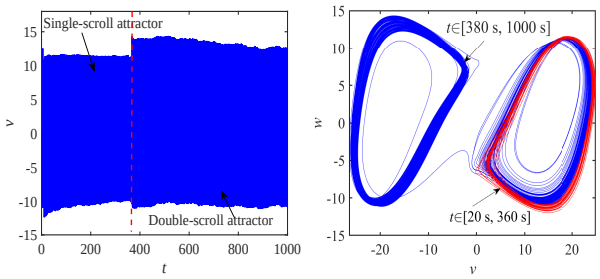


**Fig. 23** The phenomenon of transient chaos when $c = 1.97$. **a** time-domain trajectory in the interval of [0 s, 1000s]; **b** the phase diagram when $t \in [20s, 360s]$ and $t \in [380s, 1000s]$

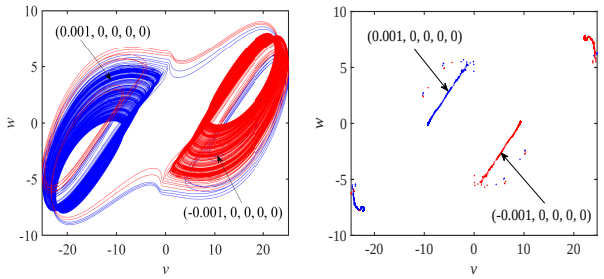


**Fig. 25** The coexisting phenomenon of steady-state chaos accompanied by burst period plotted for $b = 0.65$ and initial conditions are $(\pm 0.001, 0, 0, 0, 0)$. **a** the phase diagram; **b** the Poincaré map

### 3.4 Steady-state chaos accompanied by burst period phenomenon

When $b$ = 0.65, the system has a strange phenomenon of steady-state chaos accompanied by burst period. Figure 24 shows the steady-state chaotic attractors with period 8 in different planes, that is, a period 8 orbits coexist in chaos.This phenomenon is sensitive to the initial values of the system. When $b$ = 0.65, the coexisting phenomenon of steady-state chaos accompanied by burst period in detail and the corresponding Poincaré map are shown in Fig. 25, where the blue attractor starts from the initial conditions of (0.001, 0, 0, 0, 0) and the red one starts from (-0.001, 0, 0, 0, 0).

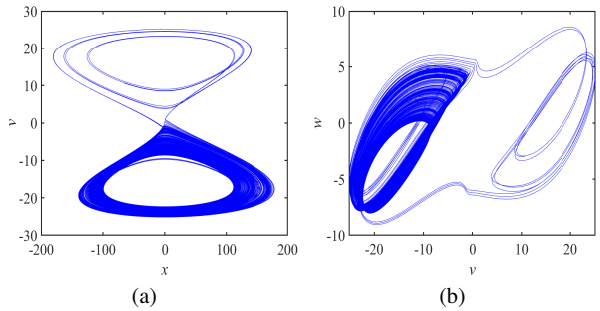


**Fig. 24** The phenomenon of steady-state chaos accompanied by burst period when $b = 0.65$

## 4 Conclusion

In this paper, a novel memcapacitor based on SBT memristor is proposed. Then, a fifth-order chaotic circuit based on this memcapacitor is designed. The characteristics of the circuit are analyzed by using the dynamics methods. With the changing of initial conditions ($x(0)$, $y(0)$, $z(0)$, $w(0)$, $v(0)$), the system is always chaotic and produes a wealth of coexisting attractors. With the changing of system parameters, the system generates complex dynamic behaviors such as transient chaos, steady-state chaos accompanied by burst period.The proposed memcapacitor and memristor chaotic circuit in this paper enriches the application of memcapacitor and memristor in high-order circuits, and expands the research methods of memcapacitor in chaotic circuits.

## Acknowledgment

This work was supported by the National Natural Science Foundation of China (Grant Nos.61703246, 61703247), the Qingdao Science and Technology Plan Project (Grant Nos. 19-6-2-2-cg), and the Elite Project of Shandong University of Science and Technology.

## References

1. Chua, L.O.: Memristor-the missing circuit element. IEEE Trans. Circuit Theory 18, 507-519 (1971)
2. Strukov, D.B., Snider, G.S., Stewart, D.R., Williams, R.S.: The missing memristor found. Nature 453, 80-83 (2008)
3. Di Ventra, M., Pershin, Y.V., Chua, L.O.: Circuit elements with memory: memristors, memcapacitors, and meminductors. Proc. IEEE 97, 1717-1724 (2009)
4. Yin, Z., Tian, H., Chen, G., Chua, L.O.: What are memristor, memcapacitor, and meminductor? IEEE Trans. Circuits Syst. II 62, 402-406 (2015)
5. Guo, M., Gao, Z.H., Xue, Y.B., Dou, G., Li, Y.X.: Dynamics of a physical SBT memristor-based Wien-bridge circuit. Nonlinear Dyn. 93, 1681-1693 (2018)

6. Guo, M., Xue, Y.B., Gao, Z.H., Zhang, Y.M., Dou, G., Li, Y.X.: Dynamic analysis of a physical SBT memristor-based chaotic circuit. Int. J. Bifurc. Chaos 27, 1730047 (2017)
7. Sun, J.W., Han, G.Y., Wang, Y.F.: Dynamical analysis of memcapacitor chaotic system and its image encryption application. Int. J. Control Autom. Syst. 18(X), 1-8 (2020)
8. Dou, G., Duan, H.Y., Yang, W.Y., Yang, H., Guo, M., Li, Y.X.: Effects of initial conditions and circuit parameters on the SBT-memristor-based chaotic circuit. Int. J. Bifurc. Chaos 29, 1950171 (2019)
9. Fitch, A.L., Iu, H.H.C., Yu, D.S.: Chaos in a memcapacitor based circuit. In: IEEE International Symposium on Circuits and Systems (ISCAS), pp. 482-485 (2014)
10. Sabarathinam, S., Volos, C.K., Thamilmaran, K.: Implementation and study of the nonlinear dynamics of a memristor-based duffing oscillator. Nonlinear Dyn. 87, 37-49 (2017)
11. Guo, M., Zhang, M., Dou, M.L., Dou, G., Li, Y.X.: Dynamics of the two-SBT-memristor-based chaotic circuit. Chin. Phys. B. 29(11), 110505 (2020)
12. Li, H.M., Yang, Y.F., Li, W., He, S.B., Li, C.L.: Extremely rich dynamics in a memristor-based chaotic system. Eur. Phys. J. Plus 135, 579 (2020)
13. Ma, X.J., Mou, J., Liu, J., Ma, C.G., Yang, F.F., Zhao, X.: A novel simple chaotic circuit based on memristor-memcapacitor. Nonlinear Dyn. 100, 2859-2876 (2020)
14. Wang, W., Zeng, Y.C., Sun, R.T.: Research on a six-order chaotic circuit with three memristors. Acta Phys. Sin. 66, 040502 (2017)
15. Guo, M., Yang, W.Y., Xue, Y.B., Gao, Z.H., Yuan, F., Dou, G., Li, Y.X.: Multistability in a physical memristor-based modified Chua's circuit. Chaos 29, 043114 (2019)
16. Lin, H., Wang, C., Tan, Y.: Hidden extreme multistability with hyperchaos and transient chaos in a hopfield neural network affected by electromagnetic radiation. Nonlinear Dyn. 99(3), 2369-2386 (2020)
17. Dou, G., Yang, H., Gao, Z.H., Li, P., Dou, M.L., Yang, W.Y., Guo. M., Li, Y.X.: Coexistence phenomena of a physical SBT memristor-based chaotic circuit. Int. J. Bifurc. Chaos 30, 2030043 (2020)
18. Wang, X., Yu, J., Jin, C., Iu, H.H.C., Yu, S.: Chaotic oscillator based on memcapacitor and meminductor. Nonlinear Dyn. 102, 2945-2950 (2020)
19. Biolek, D., Biolkova, V., Kolka, Z.: Mutators simulating memcapacitors and meminductors. In: APCCAS, pp. 800-803 (2010)
20. Pershin, Y.V., Ventra, M.D.: Memristive circuits simulate memcapacitors and meminductors. Electron. Lett. 46, 517-518 (2010)
21. Wang, X.Y., Fitch, A.L., Iu, H.H.C., Qi, W.G.: Design of a memcapacitor emulator based on a memristor. Phys. Lett. A 376, 394-399 (2014)
22. Yu, D.S., Liang, Y., Iu, H.H.C., Chua, L.O.: A universal mutator for transformations among memristor, memcapacitor, and meminductor. IEEE Trans. Circuits Syst. II, Exp. Briefs 61(10), 758-762 (2014)
23. Pershin, Y.V., Ventra, M.D.: Emulation of floating memcapacitors and meminductors using current conveyors. Electron. Lett. 47(4), 243-244 (2011)
24. Fouda, M.E., Radwan, A.G.: Charge controlled memristor-less memcapacitor emulator. Electron. Lett. 48(23), 1454-1455 (2012)
25. Wang, G.-Y., Cai, B.-Z., Jin, P.-P., Hu, T.-L.: Memcapacitor model and its application in a chaotic oscillator. Chin. Phys. B 25(1), 010503 (2016)
26. Akgul, A.: Chaotic oscillator based on fractional order memcapacitor. J. Circuits Syst. Comput. 28(14), 1950239 (2019)
27. Zhou, W., Wang, G.Y., Iu, H.H.C., Shen, Y.R., Liang, Y.: Complex dynamics of a non-volatile memcapacitor-aided hyperchaotic oscillator. Nonlinear Dyn. 100, 3937-3957 (2020)
28. Zhao, Q., Wang, C., Zhang, X.: A universal emulator for memristor, memcapacitor, and meminductor and its chaotic circuit. Chaos 29(1), 013141 (2019)
29. Flak, J., Lehtonen, E., Laiho, M., Rantala, A., Prunnila. M., Haatainen, T.: Solid-state memcapacitive device based on memristive switch. Semicond. Sci. Technol. 29, 104012(2014)
30. Zhang, Y.M., Dou, G., Sun, Z., Guo, M., Li, Y.X.: Establishment of physical and mathematical models for $Sr_{0.95}Ba_{0.05}TiO_3$ memristor. Int. J. Bifurc. Chaos 27(9), 1750148 (2017)
31. Dou, G., Yu, Y., Guo, M., Zhang, Y.-M., Sun, Z., Li, Y.-X.: Memristive behavior based on Ba-doped $SrTiO_3$ films. Chin. Phys. Lett. 34, 038502 (2017)

# Figures

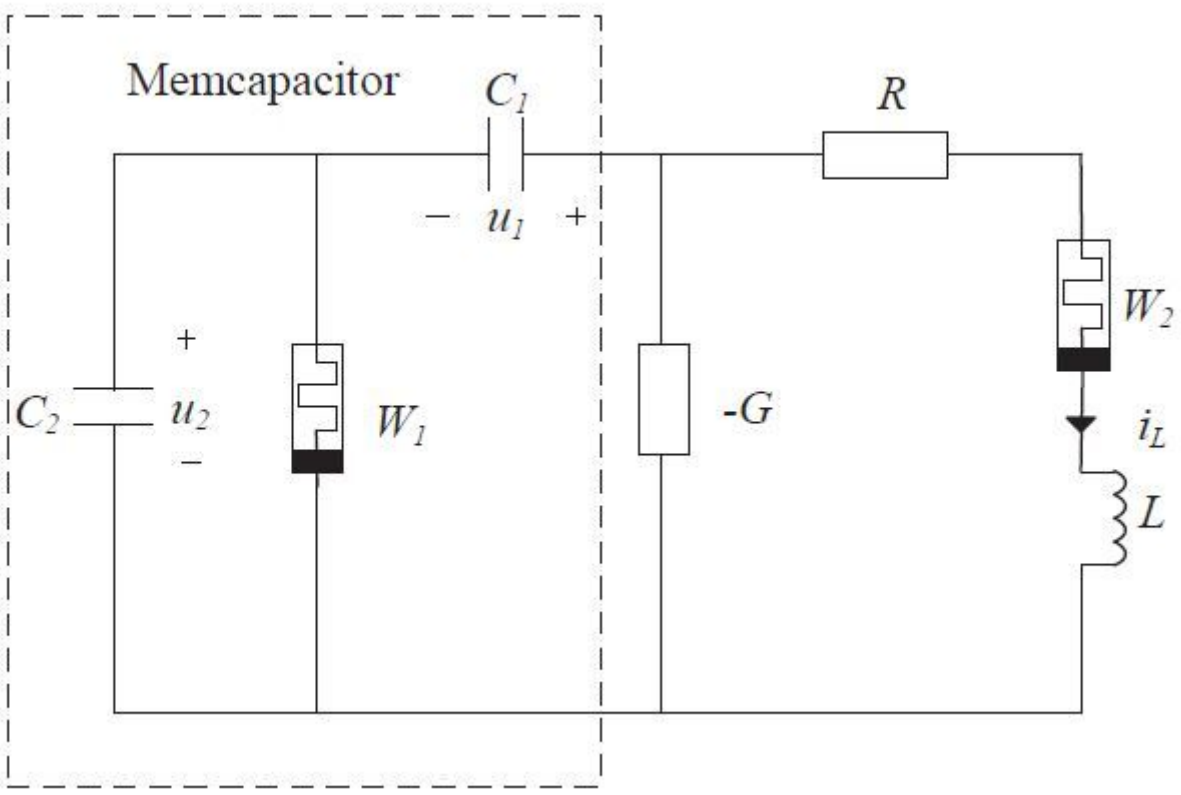


**Figure 1**

please see the manuscript file for the full caption

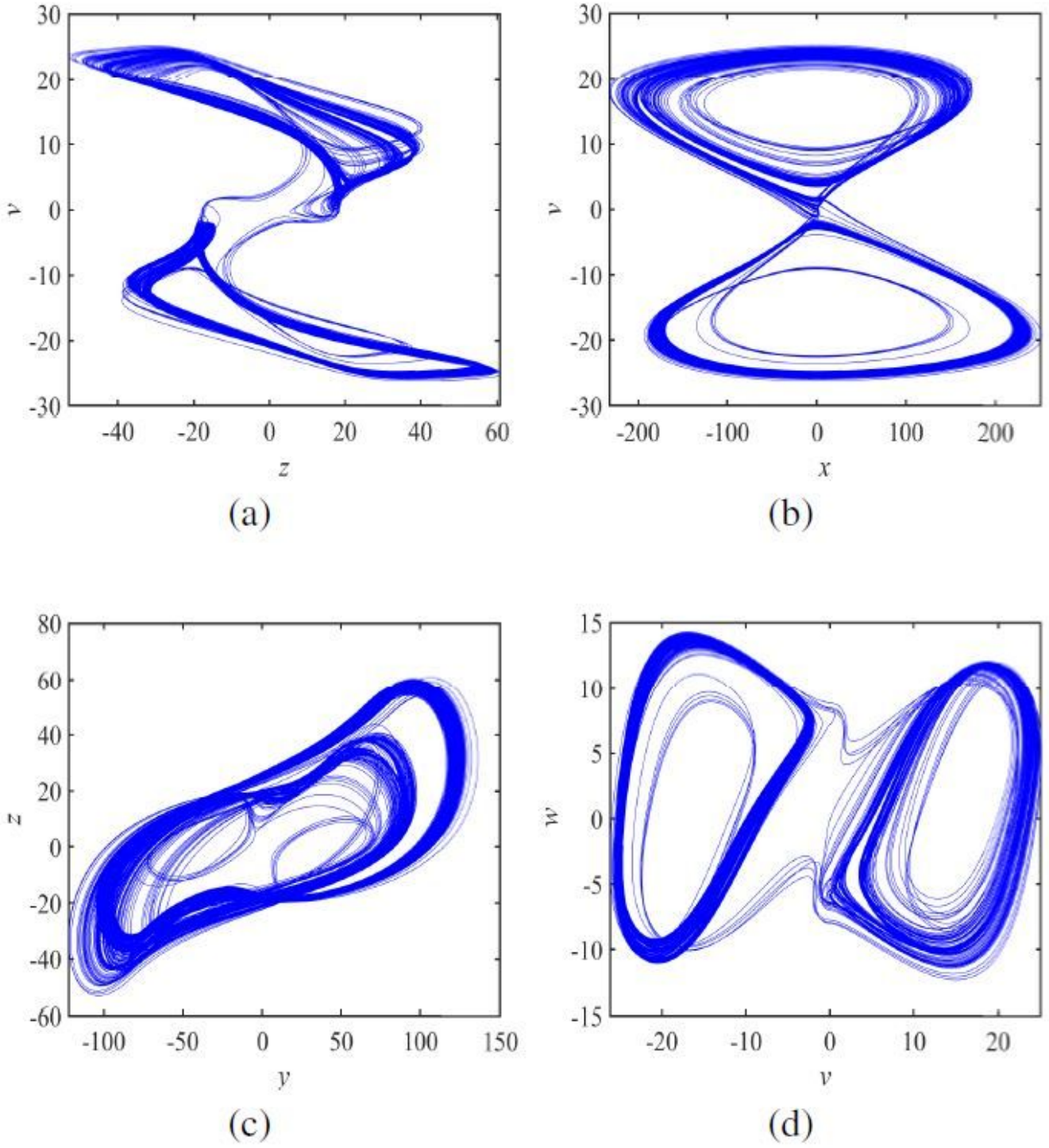


**Figure 2**

The typical chaotic attractor of Fifth-order chaotic circuit

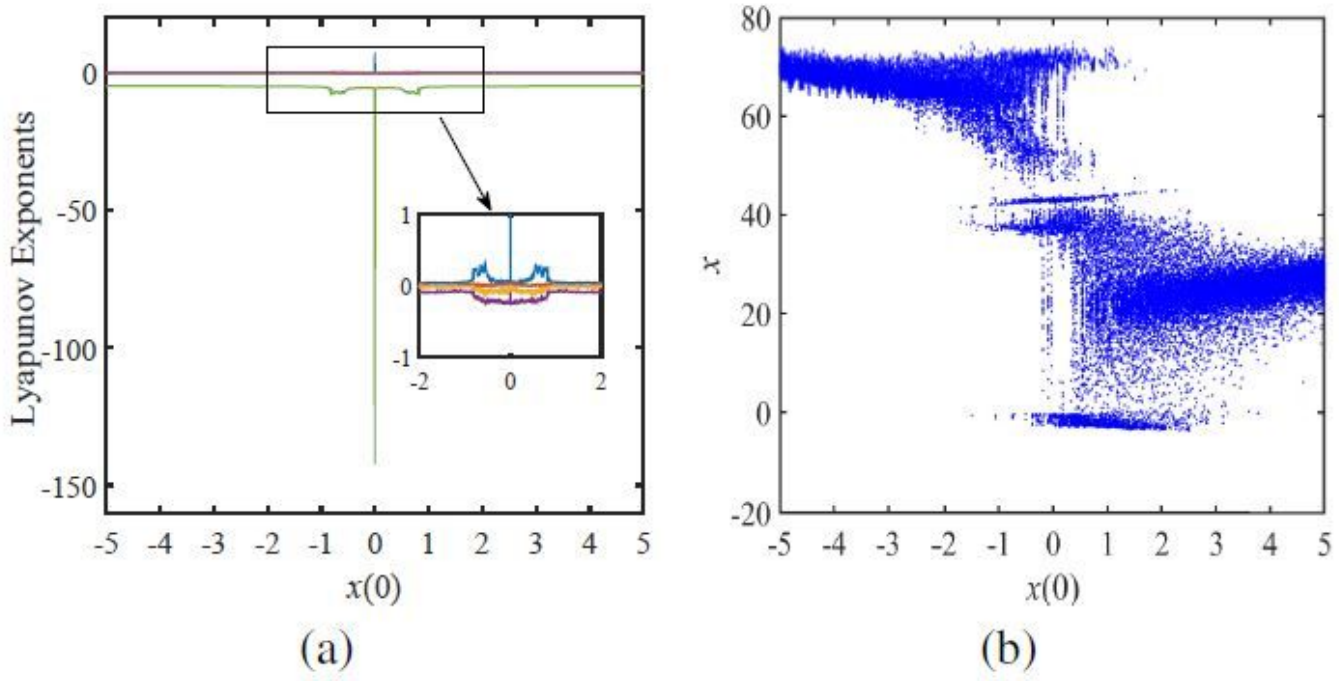


**Figure 3**

please see the manuscript file for the full caption

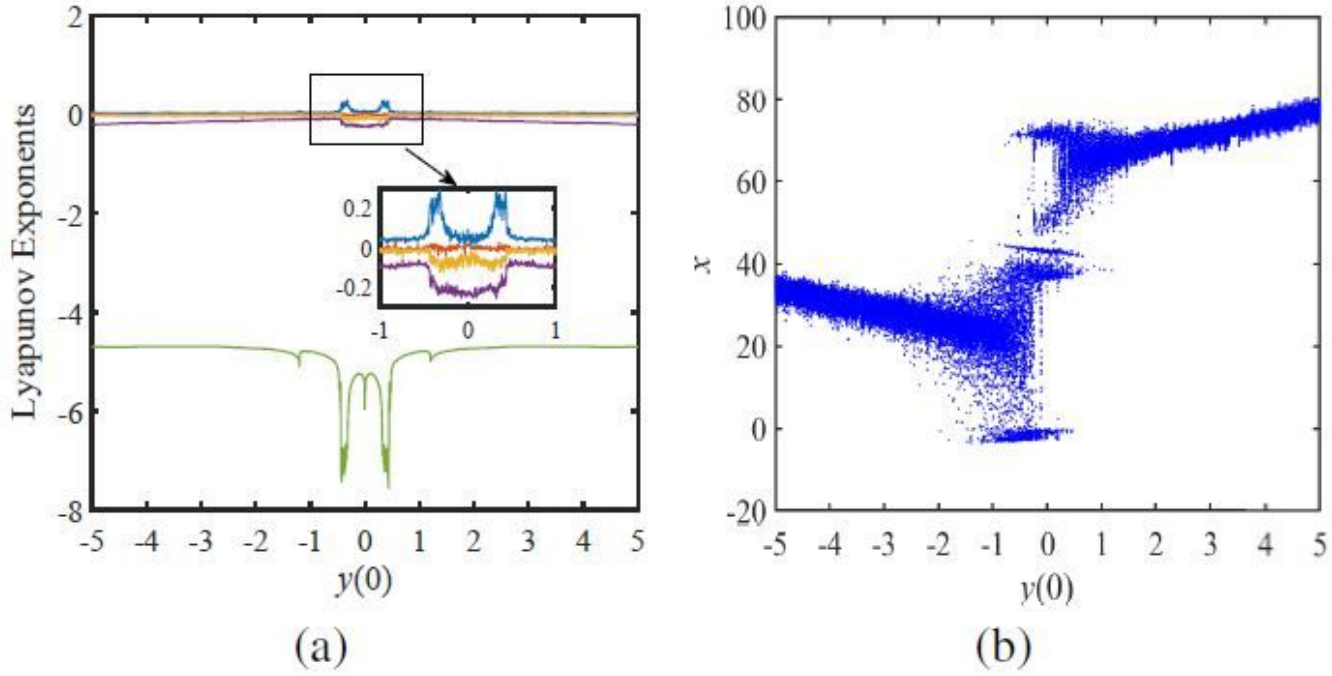


**Figure 4**

a Lyapunov exponents spectrum and b bifurcation diagram varying with the initial state y(0)

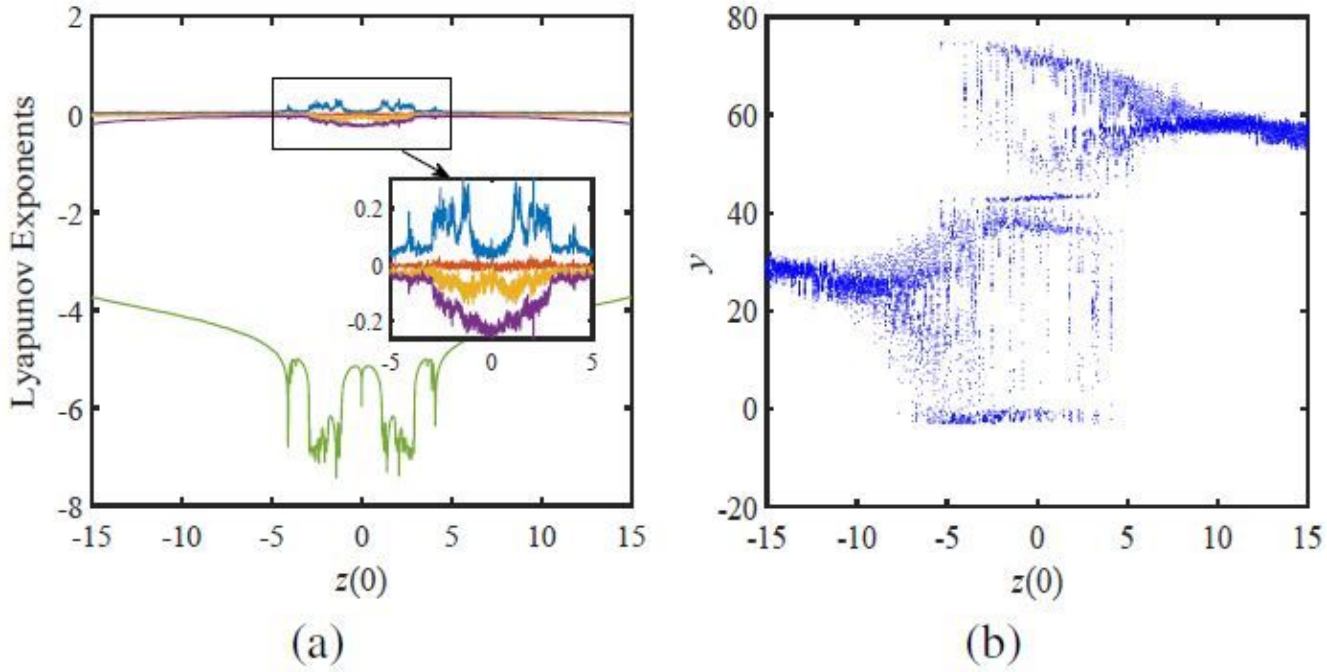


**Figure 5**

a Lyapunov exponents spectrum and b bifurcation diagram varying with the initial state z(0)

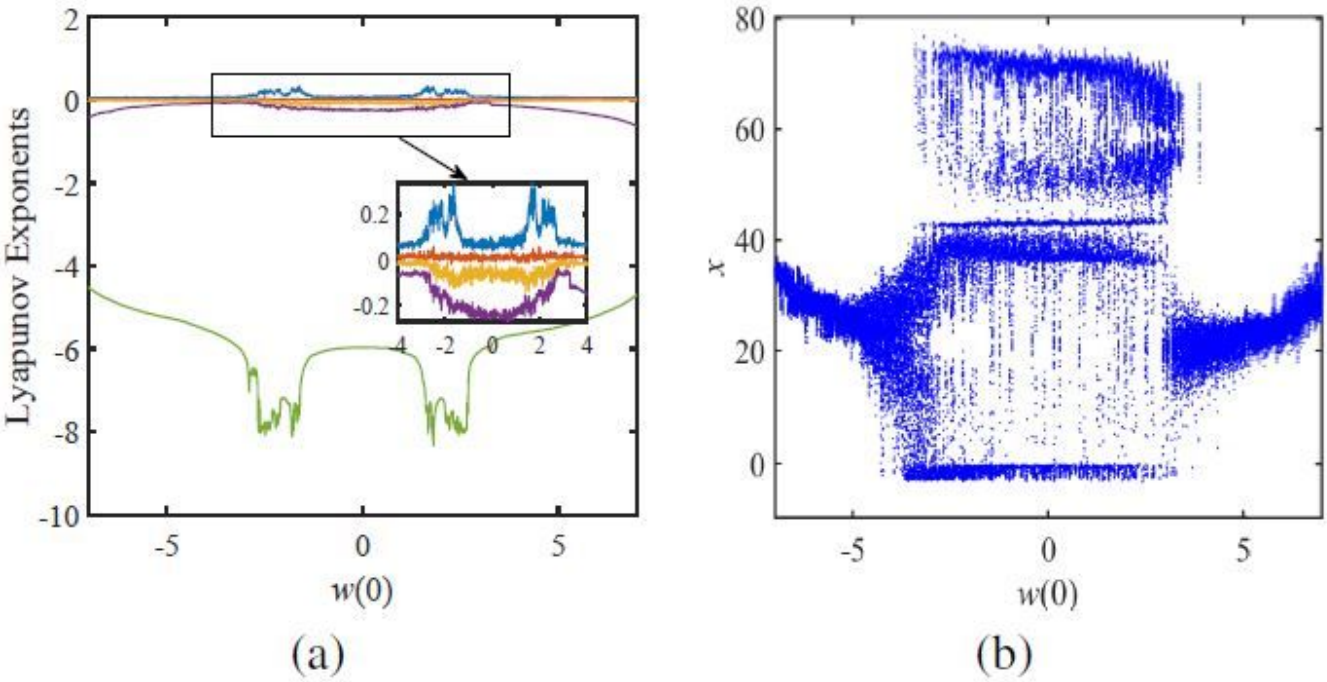


**Figure 6**

please see the manuscript file for the full caption

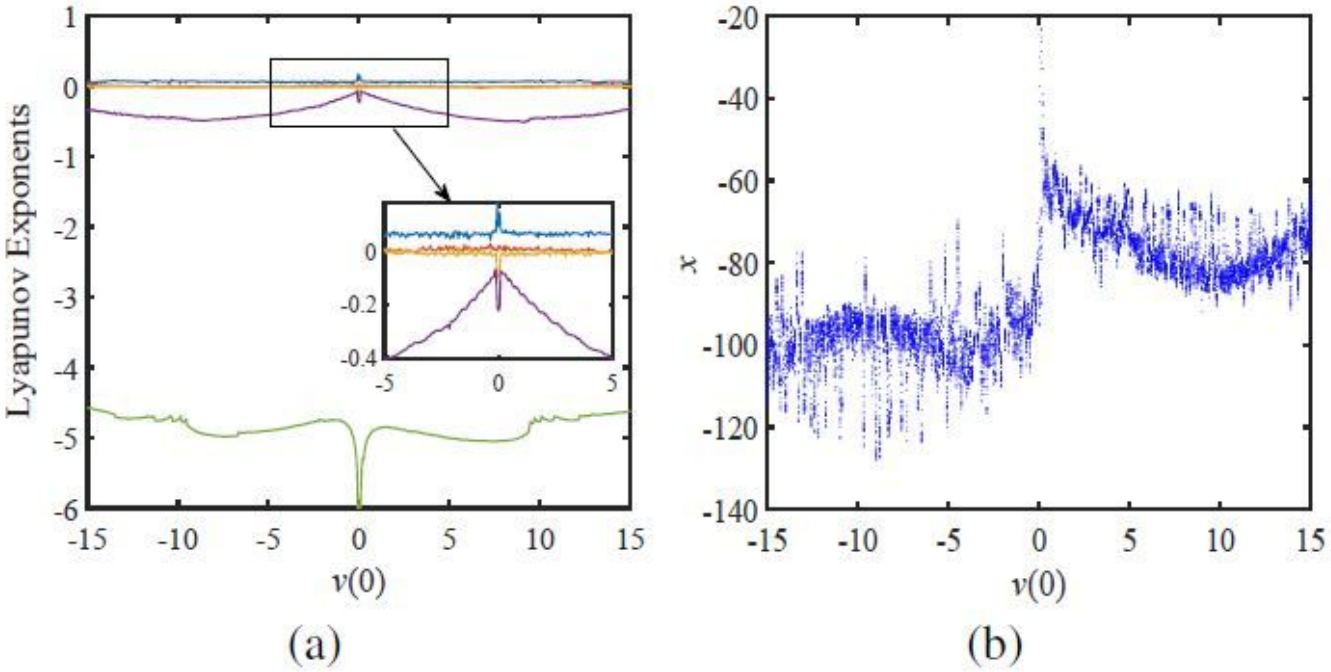


**Figure 7**

please see the manuscript file for the full caption

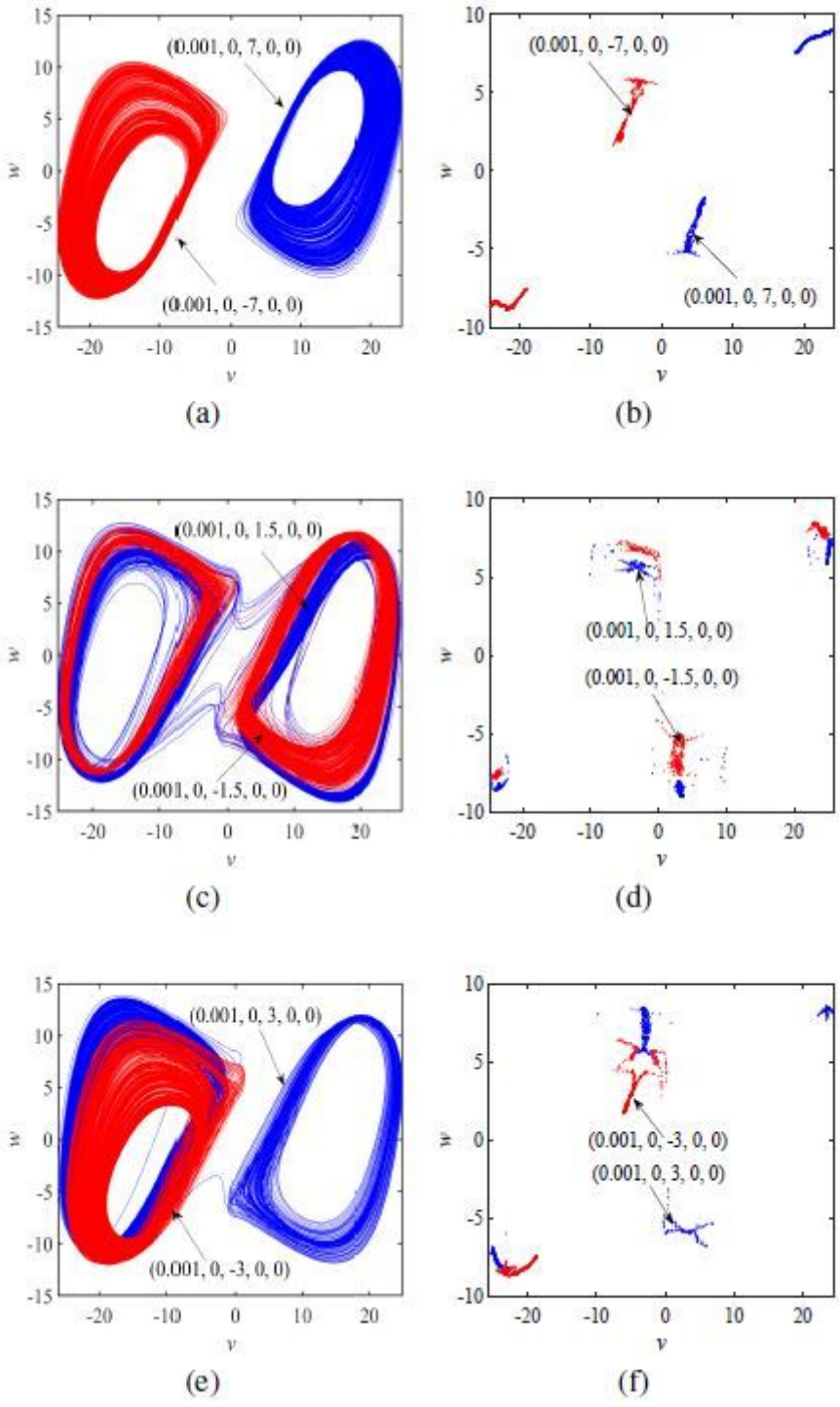


## Figure 8

please see the manuscript file for the full caption

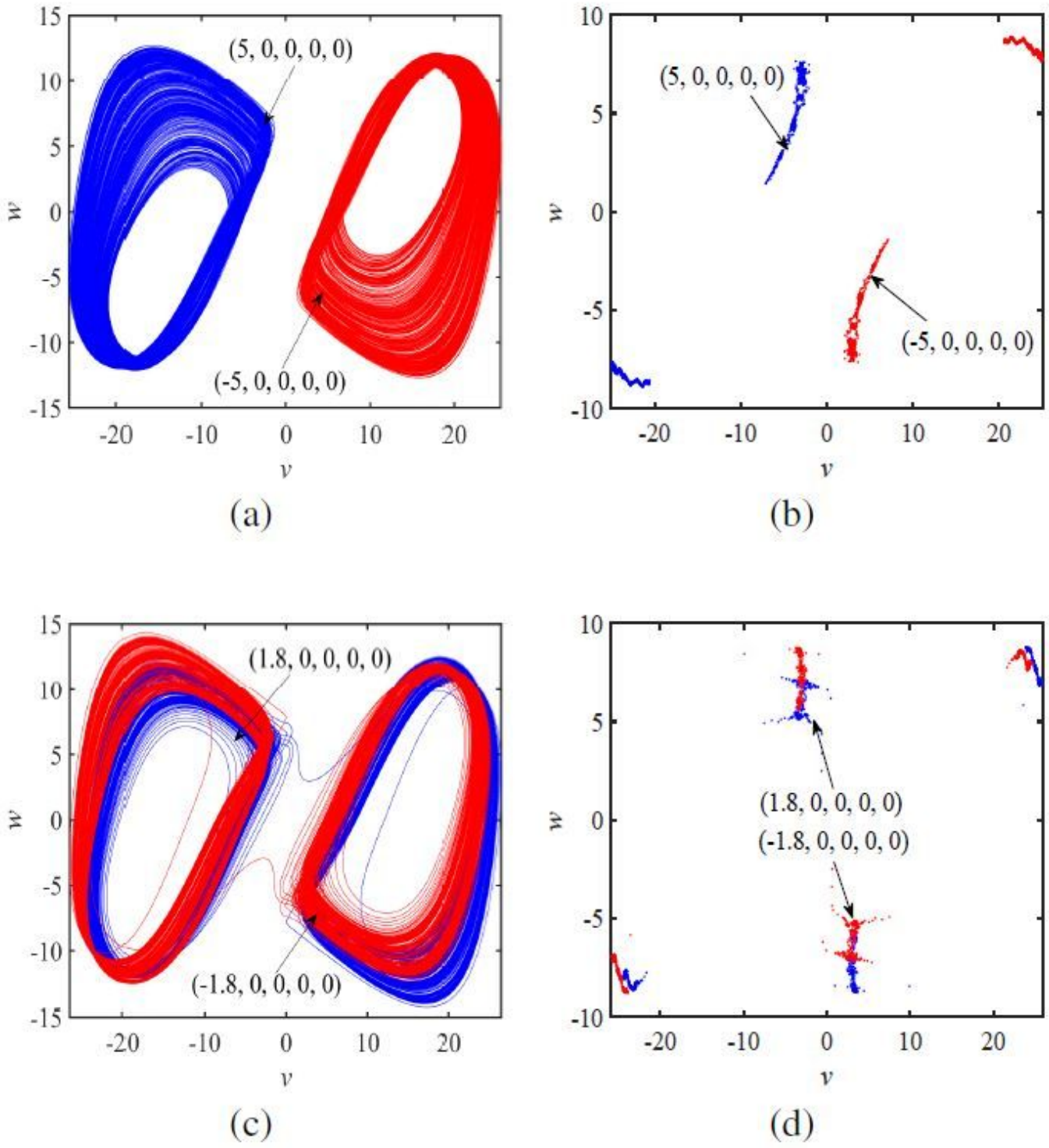


**Figure 9**

please see the manuscript file for the full caption

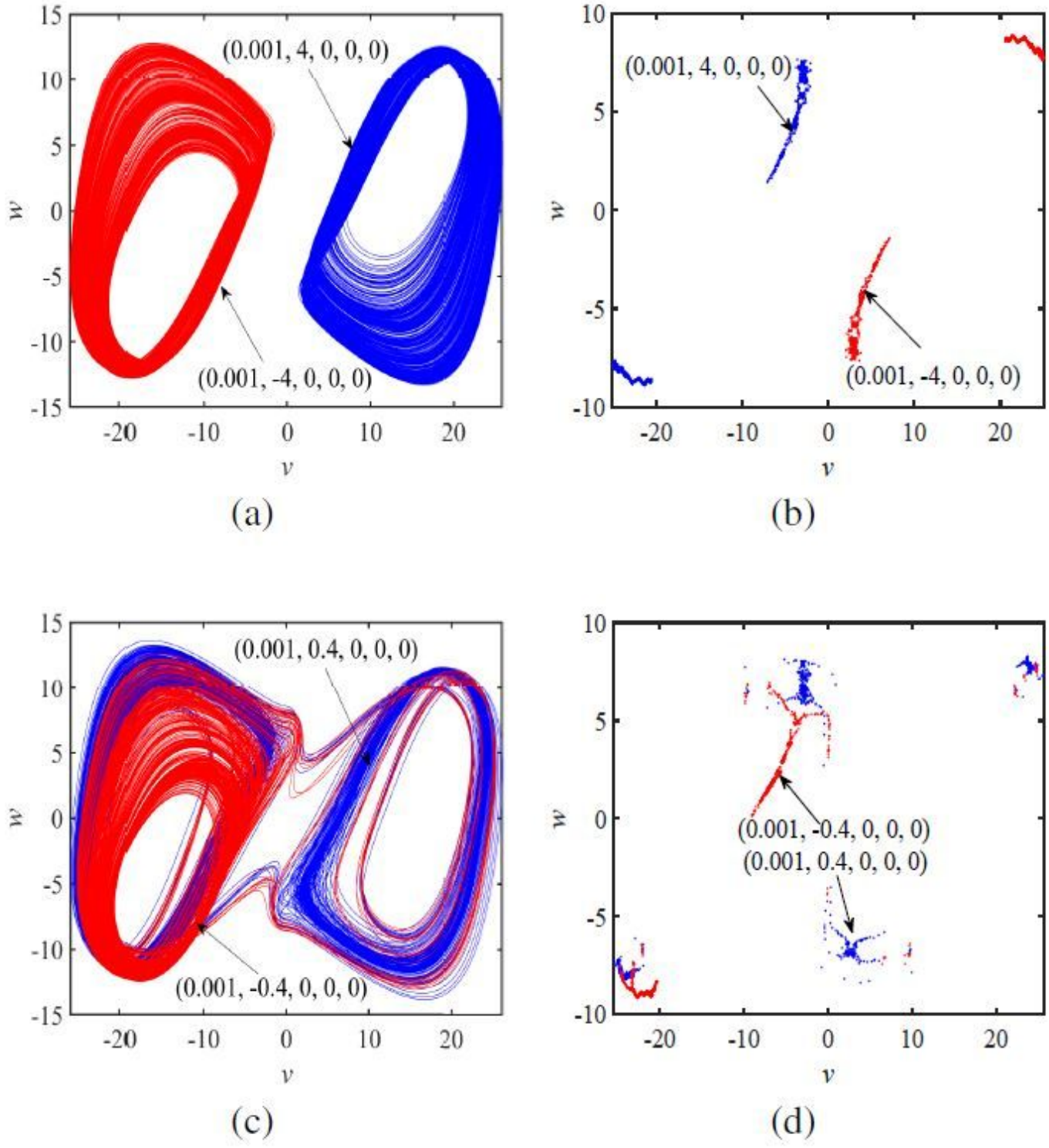


**Figure 10**

please see the manuscript file for the full caption

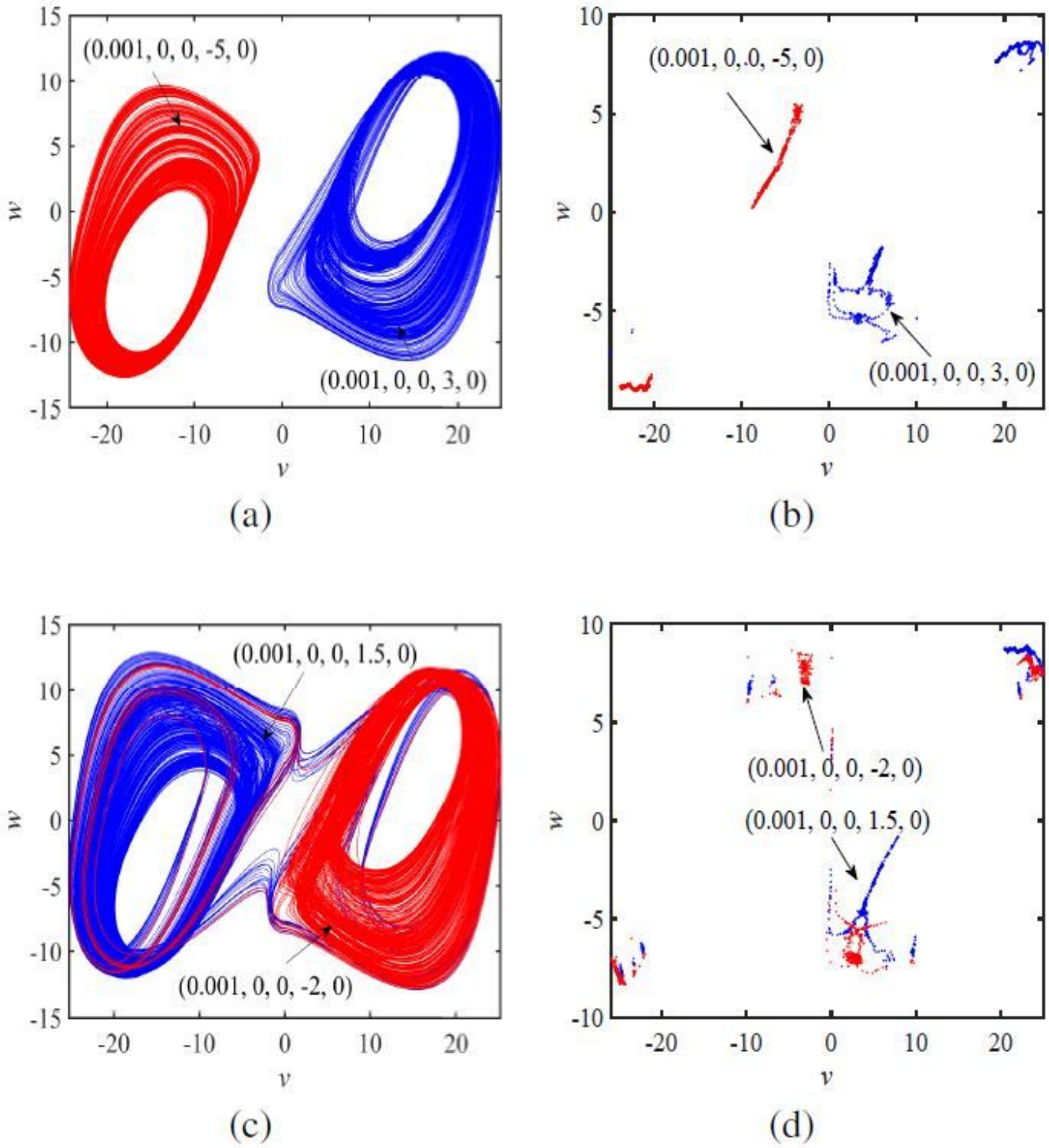


**Figure 11**

The multistability of the circuit varying with initial conditions w(0). a the phase diagram when initial conditions are (0.001, 0, 0, 3, 0) and (0.001, 0, 0, -5, 0); b the Poincar´e map when initial conditions are (0.001, 0, 0, 3, 0) and (0.001, 0, 0, -5, 0); c the phase diagram when initial conditions are (0.001, 0, 0, 1.5, 0) and (0.001, 0, 0, -2, 0); d the Poincar´e map initial conditions are (0.001, 0, 0, 1.5, 0) and (0.001, 0, 0, -2, 0).

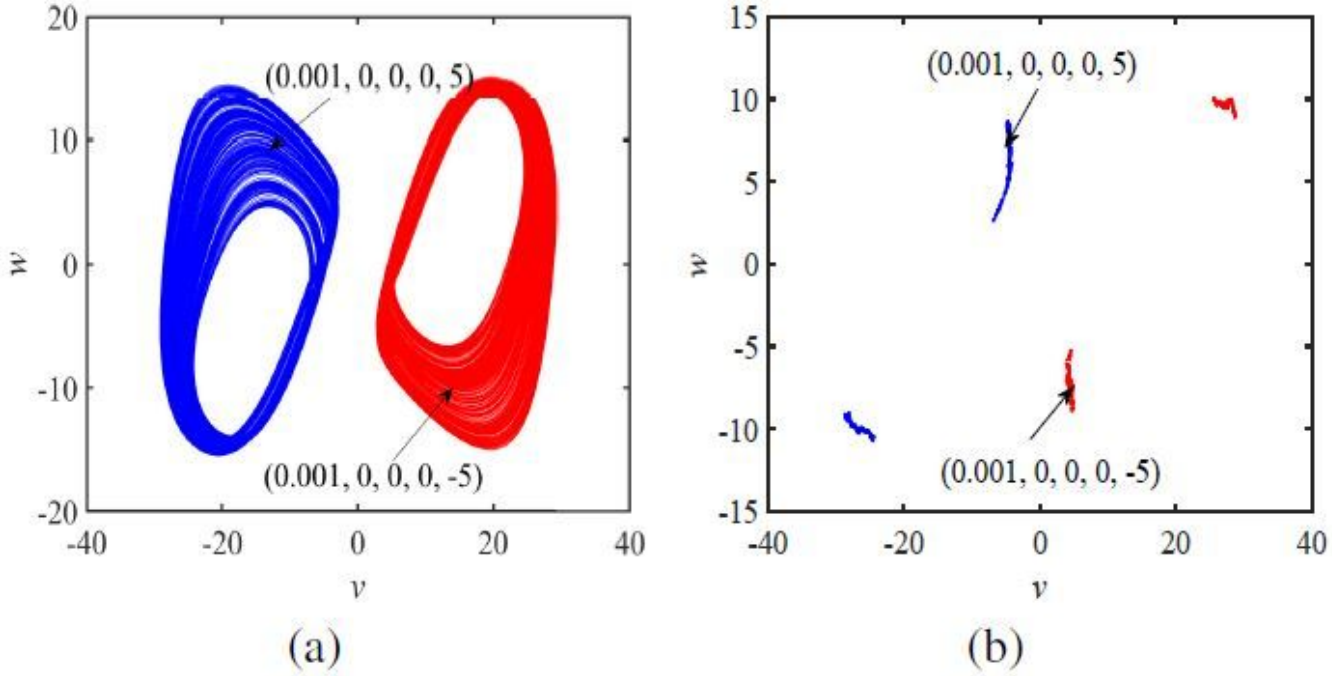


**Figure 12**

please see the manuscript file for the full caption

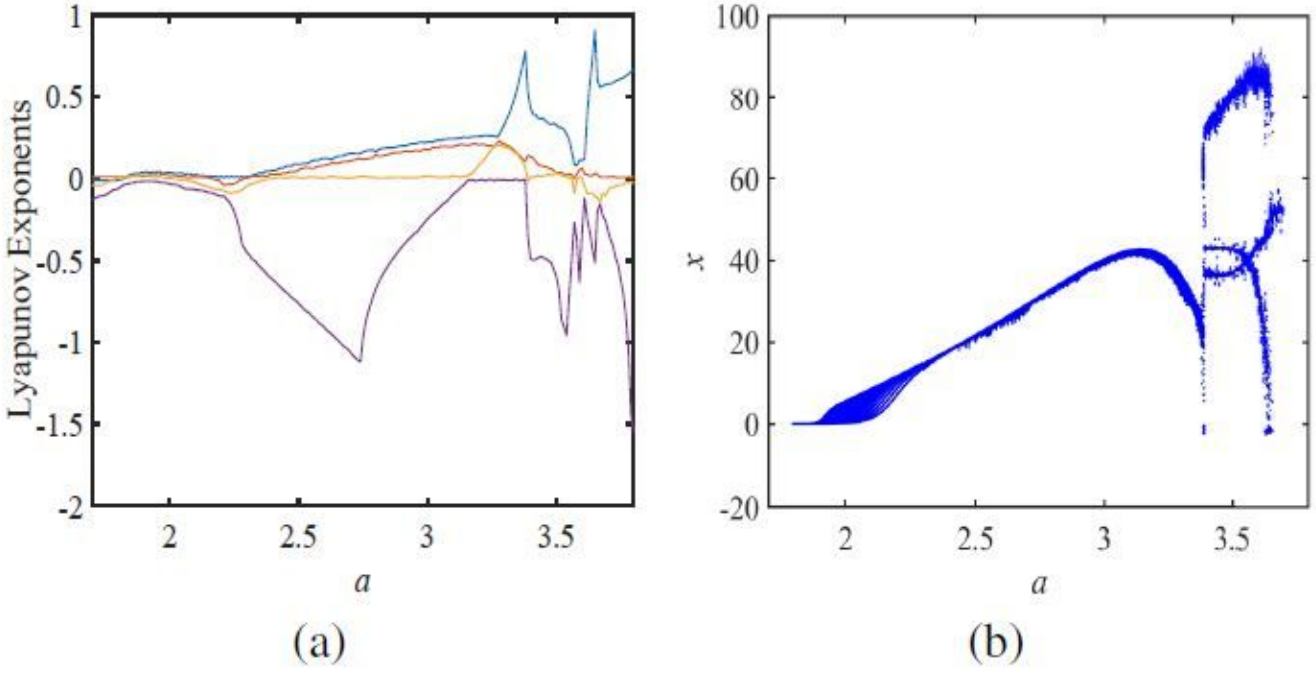


**Figure 13**

please see the manuscript file for the full caption

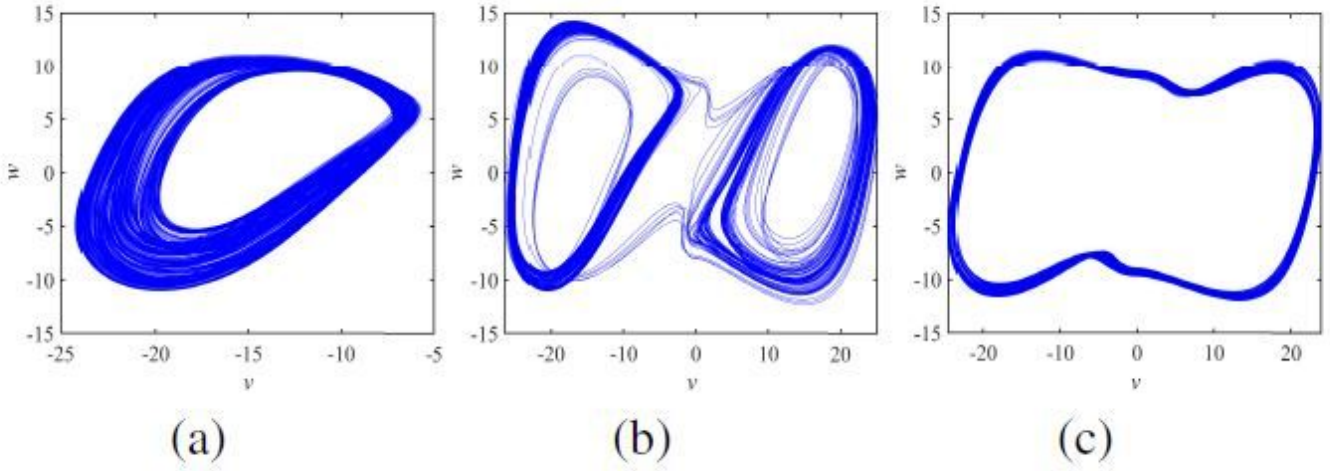


**Figure 14**

The dynamical evolution process of the system with the variety of parameter a. a α = 3:22; b α = 3:39; c α = 3:70

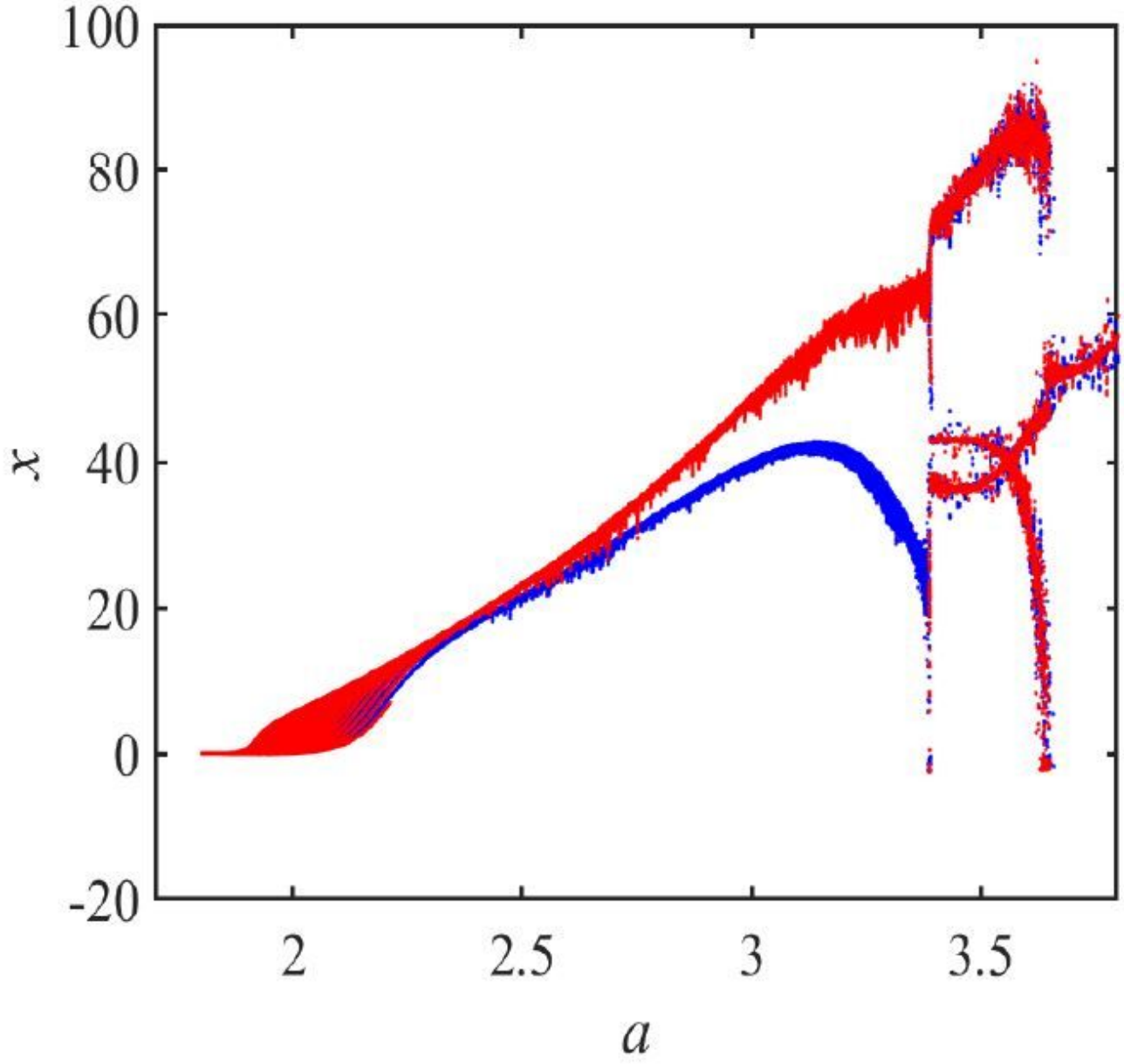


**Figure 15**

please see the manuscript file for the full caption

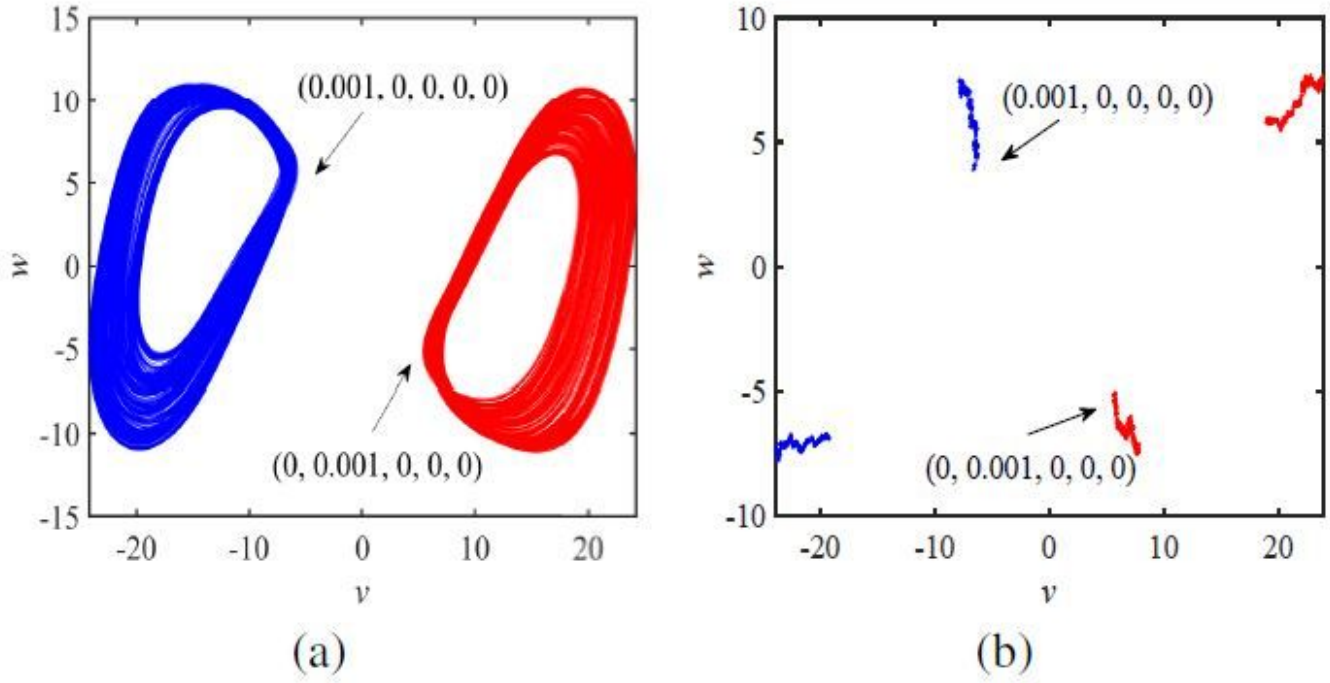


**Figure 16**

please see the manuscript file for the full caption

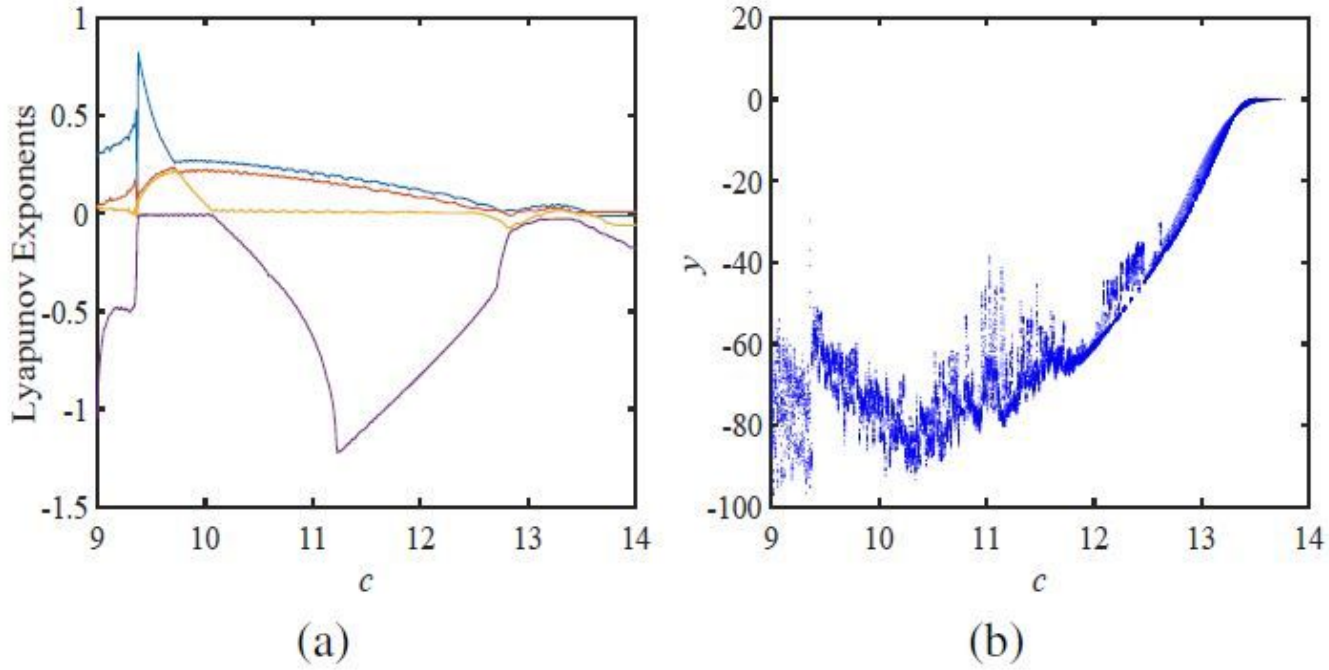


**Figure 17**

please see the manuscript file for the full caption

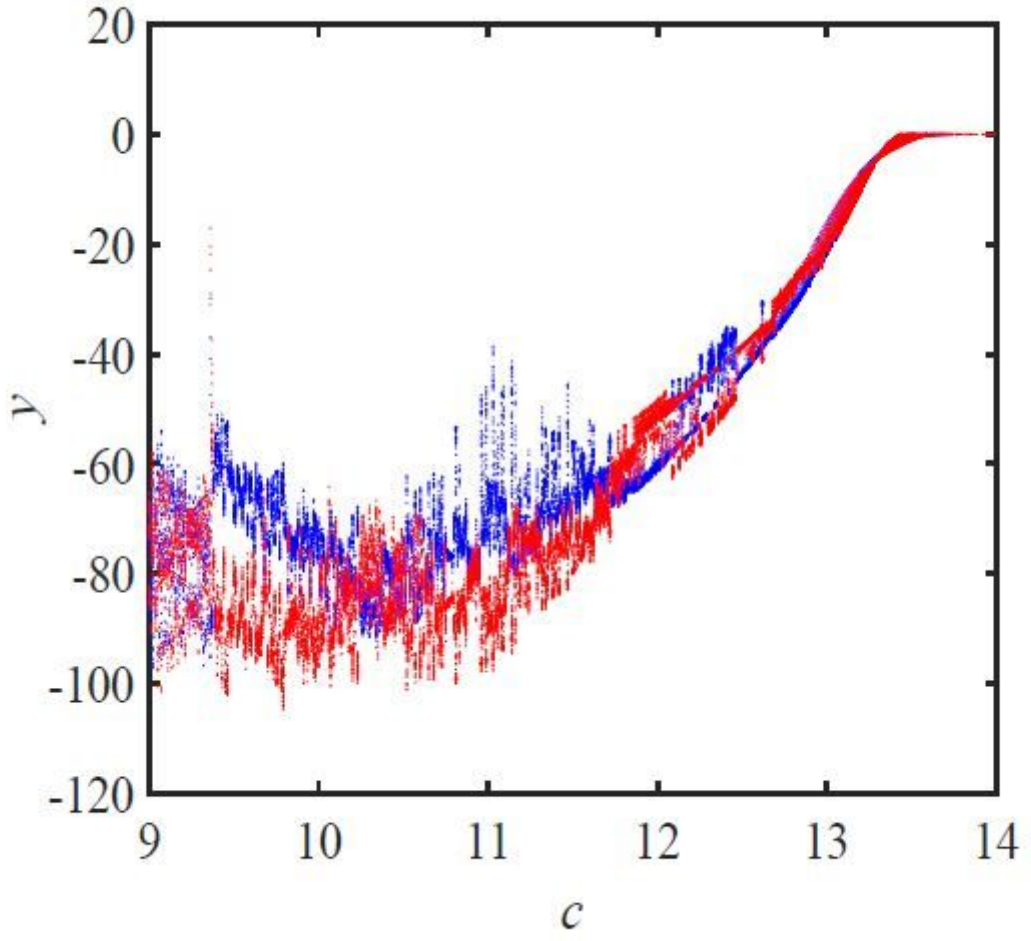


**Figure 18**

please see the manuscript file for the full caption

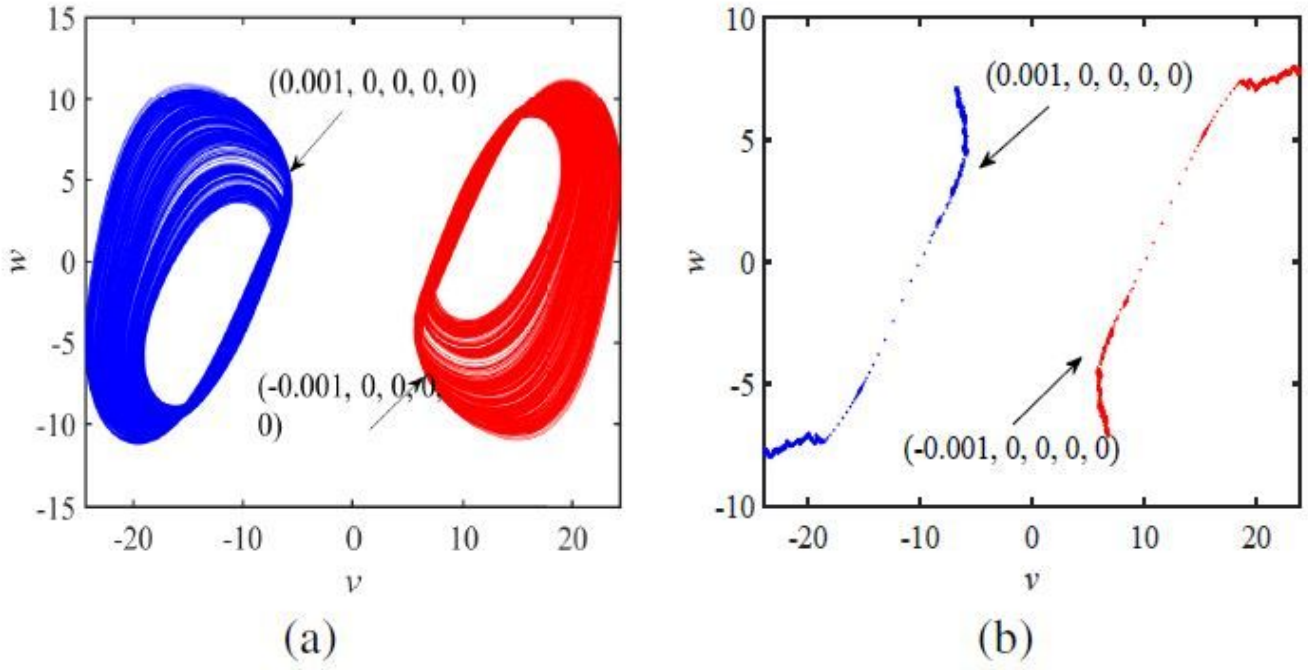


**Figure 19**

please see the manuscript file for the full caption

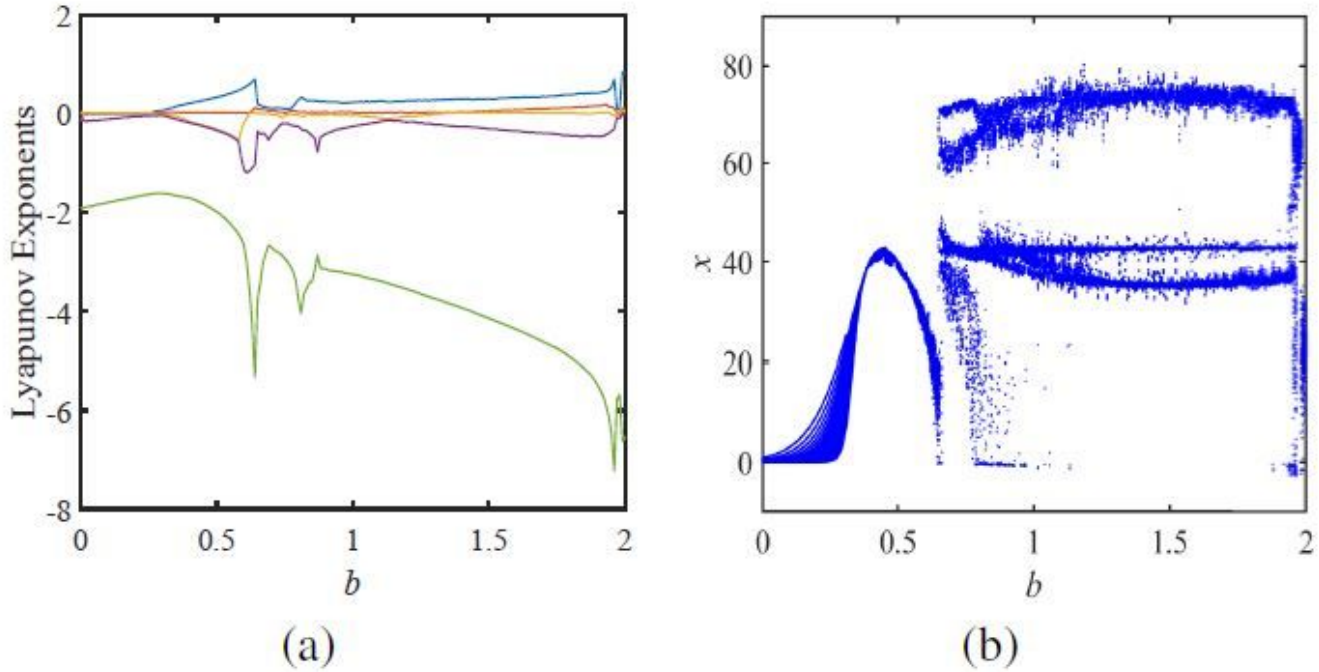


**Figure 20**

please see the manuscript file for the full caption

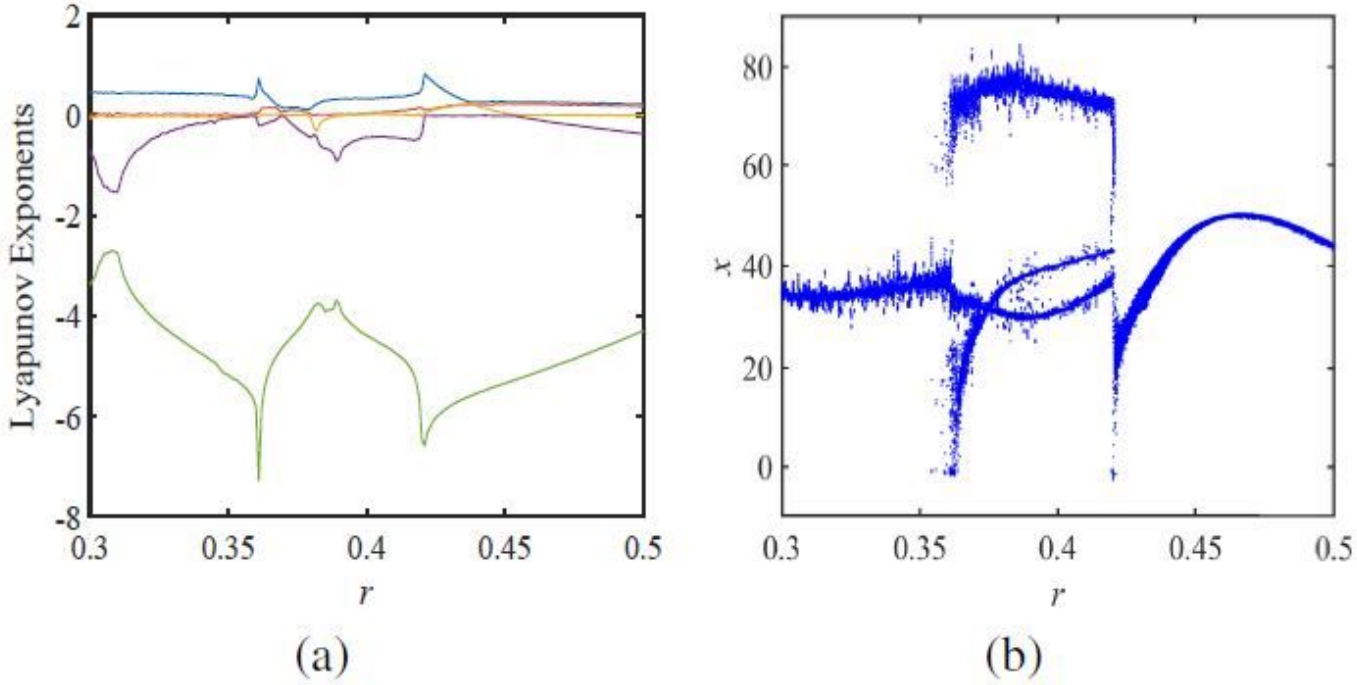


Figure 21

please see the manuscript file for the full caption

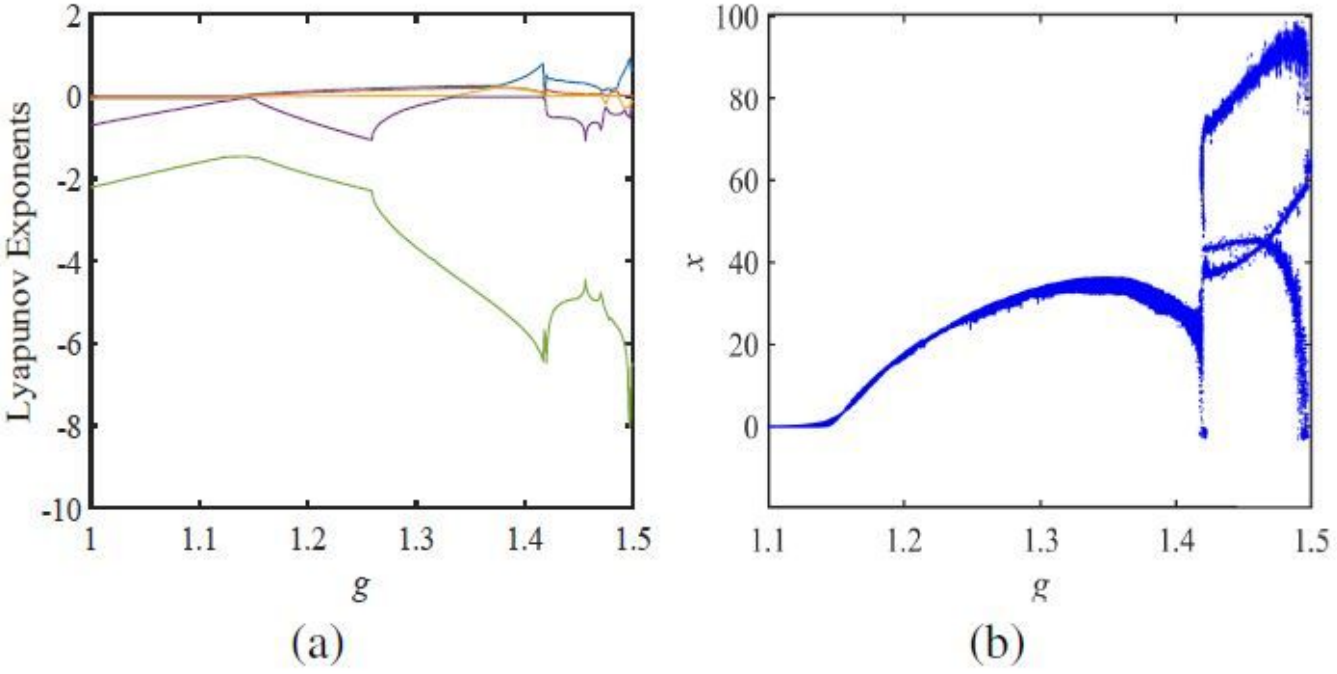


Figure 22

please see the manuscript file for the full caption

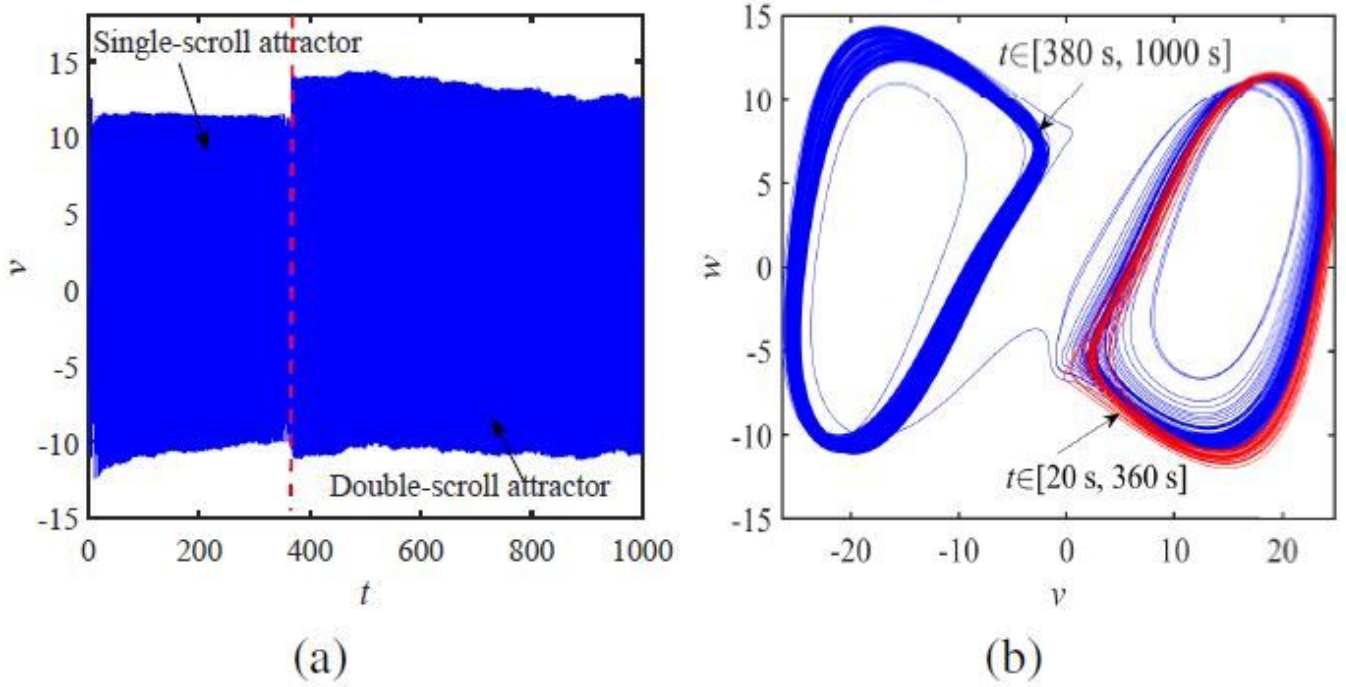


**Figure 23**

please see the manuscript file for the full caption

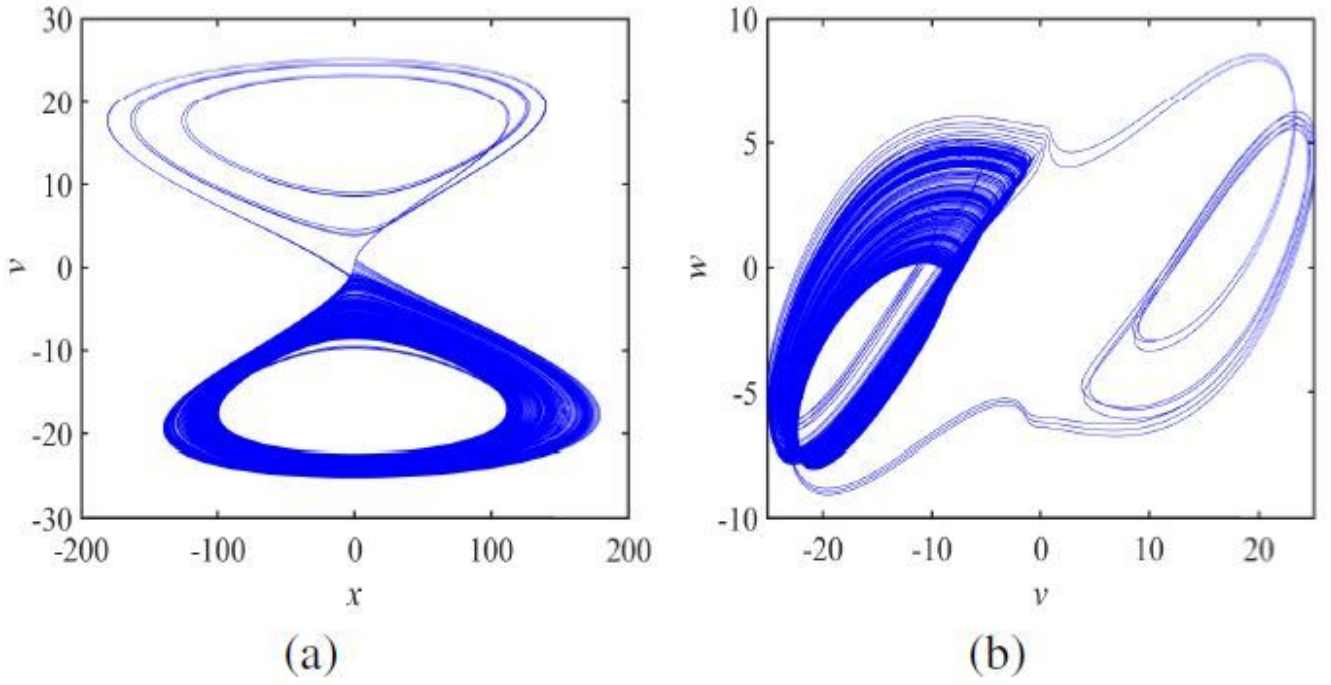

## Figure 24

please see the manuscript file for the full caption

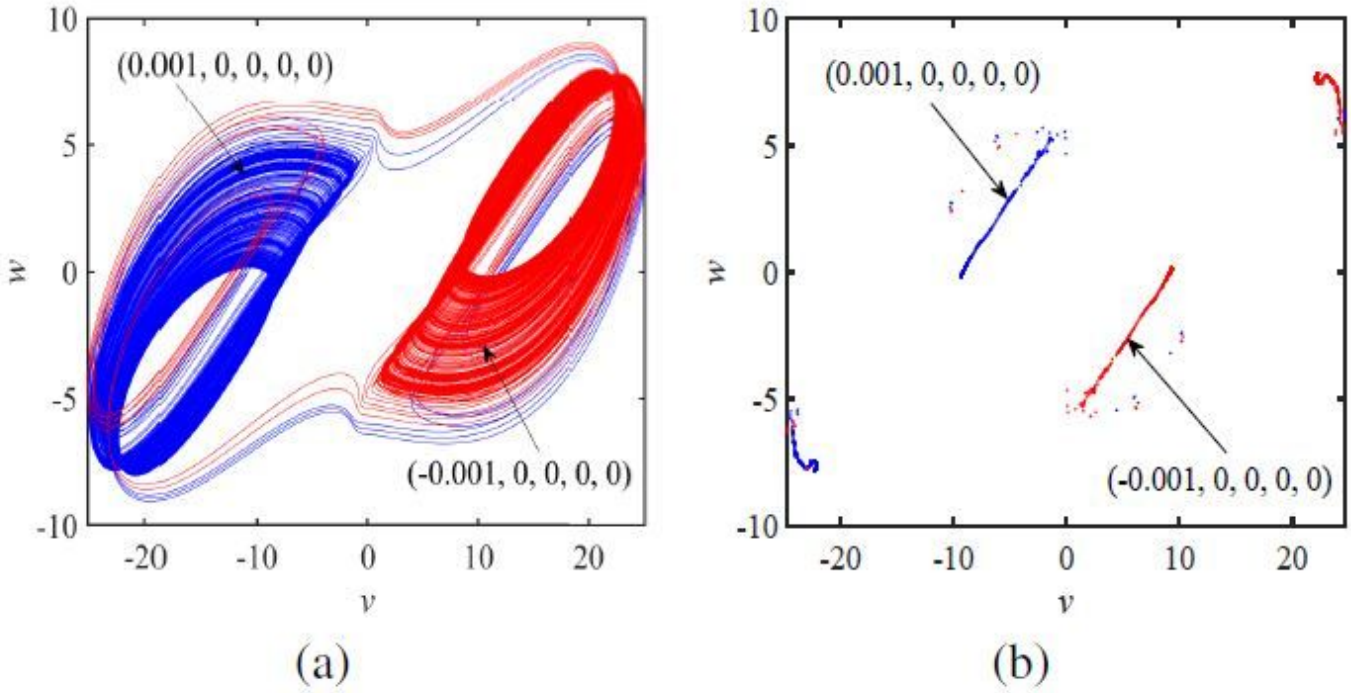


## Figure 25

please see the manuscript file for the full caption